Review

Non-Brownian diffusion in lipid membranes: Experiments and simulations☆

R. Metzler [a,b,*], J.-H. Jeon [c], A.G. Cherstvy [a]

[a] Institute for Physics & Astronomy, University of Potsdam, 14476 Potsdam—Golm, Germany
[b] Department of Physics, Tampere University of Technology, 33101 Tampere, Finland
[c] Korea Institute for Advanced Study (KIAS), Seoul, Republic of Korea

ARTICLE INFO

ABSTRACT

The dynamics of constituents and the surface response of cellular membranes—also in connection to the binding of various particles and macromolecules to the membrane—are still a matter of controversy in the membrane biophysics community, particularly with respect to crowded membranes of living biological cells. We here put into perspective recent single particle tracking experiments in the plasma membranes of living cells and supercomputing studies of lipid bilayer model membranes with and without protein crowding. Special emphasis is put on the observation of anomalous, non-Brownian diffusion of both lipid molecules and proteins embedded in the lipid bilayer. While single component, pure lipid bilayers in simulations exhibit only transient anomalous diffusion of lipid molecules on nanosecond time scales, the persistence of anomalous diffusion becomes significantly longer ranged on the addition of disorder—through the addition of cholesterol or proteins—and on passing of the membrane lipids to the gel phase. Concurrently, experiments demonstrate the anomalous diffusion of membrane embedded proteins up to macroscopic time scales in the minute time range. Particular emphasis will be put on the physical character of the anomalous diffusion, in particular, the occurrence of ageing observed in the experiments—the effective diffusivity of the measured particles is a decreasing function of time. Moreover, we present results for the time dependent local scaling exponent of the mean squared displacement of the monitored particles. Recent results finding deviations from the commonly assumed Gaussian diffusion patterns in protein crowded membranes are reported. The properties of the displacement autocorrelation function of the lipid molecules are discussed in the light of their appropriate physical anomalous diffusion models, both for non-crowded and crowded membranes. In the last part of this review we address the upcoming field of membrane distortion by elongated membrane-binding particles. We discuss how membrane compartmentalisation and the particle–membrane binding energy may impact the dynamics and response of lipid membranes. For SI: Biosimulations — This article is part of a Special Issue entitled: Biosimulations.

© 2016 Elsevier B.V. All rights reserved.

Contents

☆ For SI: Biosimulations — This article is part of a Special Issue entitled: Biosimulations.

* Corresponding author at: Institute for Physics & Astronomy, University of Potsdam, 14476 Potsdam—Golm, Germany.
E-mail address: rmetzler@uni-potsdam.de (R. Metzler).

1. Anomalous diffusion

On a molecular level the diffusion of reactive particles until their mutual encounter and subsequent reaction is a fundamental mechanism. In fact in 2016 we celebrate the centenary of Marian Smoluchowski's ground breaking mathematical analysis of this problem [1]. Most studies applying this approach to diffusion limited molecular reaction scenarios consider the Brownian motion of the reacting molecules, characterised by a Gaussian spreading of the probability density function $P(\mathbf{r}, t)$ of the particle under consideration, in conjunction with the linear time dependence

$$\langle \mathbf{r}^2(t) \rangle \simeq K_1 t \qquad (1)$$

of the mean squared displacement with diffusivity K_1, defined in terms of the probability density function $P(\mathbf{r}, t)$ to find the particle at position $\mathbf{r}$ at time t through the expectation [2]

$$\langle \mathbf{r}^2(t) \rangle = \int \mathbf{r}^2 P(\mathbf{r}, t) d^3 \mathbf{r}. \qquad (2)$$

For two molecules a and b with cumulative radius $r = r_a + r_b$ and diffusivity $K_1 = K_1^a + K_1^b$ that instantaneously react upon encounter, the Smoluchowski rate becomes $k = 4\pi K_1 r$ in three spatial dimensions [1]. This rate can only be enhanced when additional mechanisms come into play, such as active reactant transport [3,4] or the dimensional reduction due to intermittent one-dimensional sliding along the DNA of DNA binding proteins in the facilitated diffusion model [5–7].

Yet, in many systems significant deviations from the normal diffusive law Eq. (1) are routinely observed [8–10]. Methods such as fluorescence correlation spectroscopy (FCS), fluorescent recovery after photobleaching (FRAP), and single particle tracking often reveal power-law forms

$$\langle \mathbf{r}^2(t) \rangle \simeq K_\beta t^\beta \qquad (3)$$

for the mean squared displacement with the generalised diffusion coefficient K_β of physical dimension cm^2/s^β. Depending on the value of the anomalous diffusion exponent β one distinguishes between subdiffusion ($0 < \beta < 1$) and superdiffusion ($\beta > 1$) [9–14].

Such anomalous diffusion may correspond to a range of different physical processes. All of these different processes exhibit the same power-law scaling of the mean squared displacement Eq. (3), however, their other dynamic properties may differ significantly [12–14]. These properties in turn critically affect the way we need to extract parameters from measurements, and the predictions of our quantitative models for follow-up processes such as diffusion limitation of molecular reactions [12–14]. To properly identify the physical nature of an anomalous diffusion process, a range of diagnosis tools have been developed, see, for instance, [13–20]. We will comment on these issues further below.

Signatures of anomalous dynamics in molecular biological systems were already reported in the 1970s for the rebinding of ligands to myoglobin molecules [21]. With modern fluorescent methods it was later proved that the observed power-law distribution of binding times is related to the non-Brownian gating dynamics of the relative motion of two amino acids, that are distant to each other when measured along the chemical backbone of the protein [22]. Very recent supercomputing studies reveal that this anomalous relative motion in fact persists over thirteen decades in time and exhibits *ageing*: the relative motion of chemically distant amino acids in different proteins is non-stationary and is characterised by a diffusivity, that is a decaying function of time [23].

In the following, we first report examples for anomalous diffusion of the form Eq. (3) from more established bulk scenarios, in particular, from single particle tracking experiments inside living cells. Based on the physical insight provided by these studies we then turn to the corresponding scenario in effectively two-dimensional membranes. We discuss in detail results from experiments measuring the anomalous diffusion dynamics of membrane embedded proteins in living cells, before turning towards supercomputer simulations studies of simple lipid bilayer systems as well as crowded membranes (see Fig. 1). In the final part of this review we then address the consequences of membrane deformations due to binding of larger objects such as elongated viruses.

2. Volume crowding causes anomalous diffusion

The internal volume of living biological cells constitutes a highly complex environment, that is compartmentalised by membrane structures and crowded with macromolecules and structural cytoskeletal networks. Macromolecular crowding by larger biopolymers makes up a *superdense* [25] liquid modulating the kinetics of various biochemical processes in cells. Macromolecular crowding in live cells, compare Fig. 2, amounts to volume occupancies beyond 30% [26–28] and generally facilitates the association of proteins via volume exclusion effects favouring more compact states [29] and has a variety of implications [28,30–34]. In model systems, for instance, crowding was shown to influence fundamental physical processes such as polymer looping relevant to cellular processes [35–37]. Folding of proteins is similarly affected by crowding [38–42] as well as aggregation [43,44].

Macromolecular crowding in live cells strongly impacts the diffusive motion of endogenous and artificially introduced *submicron tracers*. After the report of anomalous diffusion of the subdiffusive kind with $0 < \beta < 1$ for different cell types in the pioneering works of Schwille et al. [45,46], subdiffusion was indeed measured for labelled dextran probes in living HeLa cells [47], labelled messenger RNA in *Escherichia coli* bacteria [25,48], DNA loci [48,49], labelled telomeres in human U2OS cells [50], visible lipid granules in yeast cells [51,52], insulin lipids in MIN6 cells [53], HIV-1 integrase in HeLa cells [54], and labelled viruses in HeLa cells [55], see also the systems reviewed in [9,10,13,14].

Consistent results of anomalous diffusion were obtained in artificially crowded systems [56–59]. Similar anomalous diffusion due to crowding is also observed in soft glassy systems [60]. Anomalous diffusion of submicron tracers due to caging by structural elements similar to those of the cellular cytoskeleton were studied in vitro in semiflexible actin gels [61]. Such caging-like trajectories were also observed near the colloidal glass transition [62]. In simulations of flexible gels anomalous diffusion was observed for tracer particles of similar size as the typical mesh size [63]. We note here that due to active motion such as motor driving [64–66] or cytoplasmic streaming [67] also superdiffusive motion with $\beta > 1$ of tracer particles in living cells may be observed. Recently it was demonstrated that not only the relatively large submicron probes and viruses but also much smaller green fluorescent proteins (GFPs) perform anomalous diffusion in both the cytoplasm and the nucleoplasm of living cells [68]; see Fig. 3.
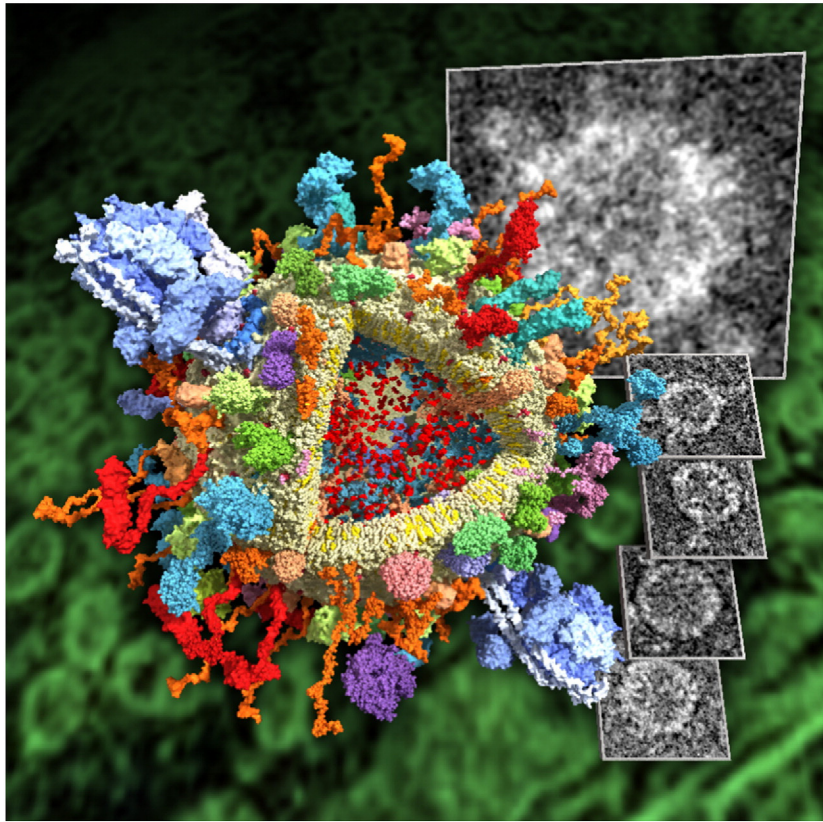
Fig. 1. Crowding of a lipid bilayer vesicle with proteins. This is a molecular model of a synaptic vesicle filled with neurotransmitters (red). The membrane (yellow) of the vesicle is packed with functional proteins, as SNARE complexes (red/orange) that help in the vesicle fusion process, and ATPases (blue), which provide the energy for the organelle. The small grey panels on the right hand side show electron microscopy images of real synaptic vesicles, the big grey image simulates how the molecular model would appear if imaged by an electron microscope. Note how massive the outside domains of the membrane embedded proteins may be. Figure courtesy H. Grubmüller [24].
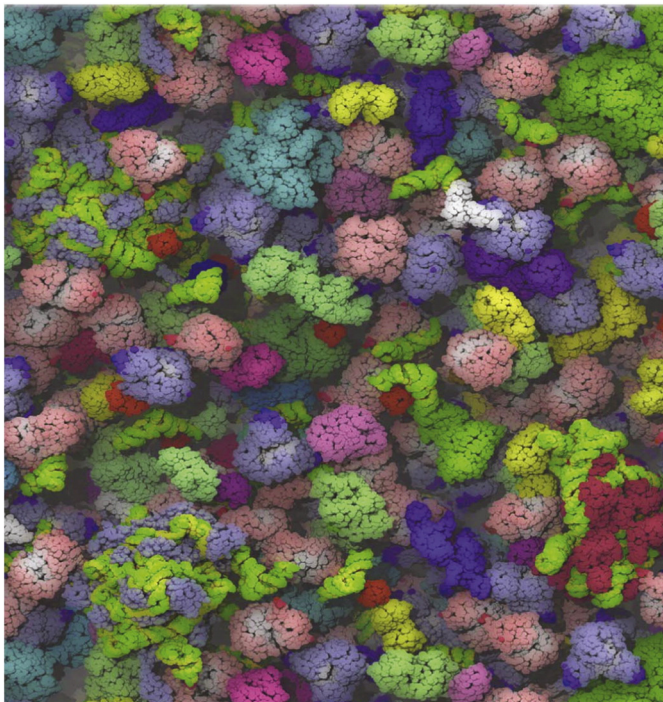
3. Time averaged observables for single particle tracking

FCS and FRAP measurements reveal ensemble averaged correlation functions, in which detailed individual molecular behaviour may be masked. In contrast, single particle tracking provides the full time series of a single traced particle. Typically only few but long particle trajectories are measured, and then evaluated in terms of the time averaged mean squared displacement [12,13]

$$\overline{\delta^2(\Delta)} = \frac{1}{T-\Delta}\int_0^{T-\Delta}(\mathbf{r}(t+\Delta)-\mathbf{r}(t))^2 dt, \qquad (4)$$

where Δ is called the lag time and T is the entire length of the trajectory (measurement time). The quantity (Eq. (4)) thus corresponds to an evaluation in terms of a sliding window of width Δ. For each Δ the information of the entire trajectory is evaluated, in contrast to the ensemble mean squared displacement Eq. (3), in which the information, at a given time, stems from a specific configuration of the system at time t. This conceptual difference between time and ensemble averaged mean squared displacements may give rise to unusual behaviours, as shown below. To obtain smoother curves often an additional average of the quantity (Eq. (4)) is taken over an ensemble of N trajectories,

Fig. 2. Macromolecular volume crowding. The image from an extensive computer study includes the 50 most abundant proteins in an *E. coli* bacteria cell [26].

$$\left\langle\overline{\delta^2(\Delta)}\right\rangle = \frac{1}{N}\sum_{i=1}^{N}\overline{\delta_i^2(\Delta)}. \qquad (5)$$
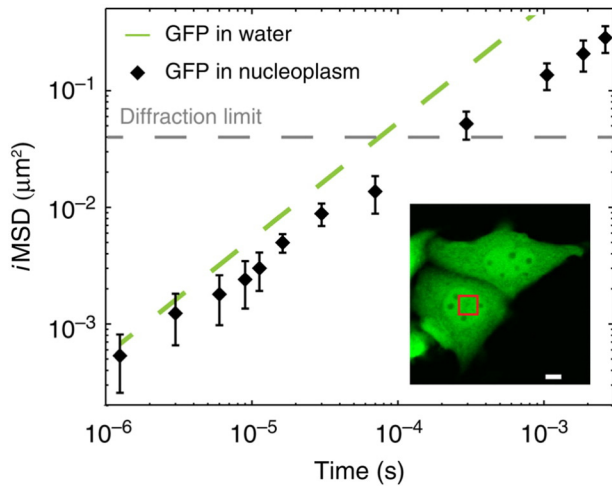
Fig. 3. Anomalous diffusion of single GFP molecules in the nucleus of living CHO cells and analysed under physiological conditions (inset) [68]. In the double logarithmic plot the slope of the mean squared displacement significantly deviates from the linear dependence of Brownian motion, over time ranges from μs and beyond ms.

Direct quantities to determine deviations from normal Brownian diffusion based on the mean squared displacement Eqs. (3), (4), and (5) include the local scaling exponent [13]

$$\beta(\text{time}) = \frac{d(\log[\text{MSD}(\text{time})])}{d(\log[\text{time}])}, \tag{6}$$

where MSD represents the respective definitions of the mean squared displacements and time stands for either regular time t in the ensemble definition Eq. (3) or the lag time Δ for the time averaged quantities. Another quantity used increasingly is the non-Gaussianity parameter as evaluated from the recorded time series [62,69,70],

$$G(\Delta) = \frac{d}{d+2} \times \frac{\left\langle \overline{\delta^4(\Delta)} \right\rangle}{\left\langle \overline{\delta^2(\Delta)} \right\rangle^2} - 1. \tag{7}$$

Here d is the dimension of the embedding space. This parameter vanishes for Gaussian processes such as Brownian motion. We also mention and quantify the displacement autocorrelation function [71]

$$C_{\delta t}(t) = \frac{1}{(\delta t)^2} \langle [\mathbf{r}(t + \delta t) - \mathbf{r}(t)] \times [\mathbf{r}(\delta t) - \mathbf{r}(0)] \rangle \tag{8}$$

evaluated along the particle trace. We will come back to this quantity below. The function $C_{\delta t}(t)$ has quite distinct properties for different anomalous diffusion processes [13], as we compare below for results of simulation for the lipid diffusion. We also mention here the van Hove correlation function, for which time averaged analogues can be efficiently determined [63].

For Brownian motion we expect that for sufficiently long measurement times T the time average Eqs. (4) and (5) provide the same information as the ensemble average Eq. (3), formally $\lim_{T\to\infty}\overline{\delta^2(\Delta)} = \lim_{T\to\infty}\langle\overline{\delta^2(\Delta)}\rangle = \langle \mathbf{r}^2(\Delta)\rangle$ [12,13]. Even for some anomalous diffusion processes such as fractional Brownian and fractional Langevin equation motion [13] this asymptotic equality is fulfilled. However, there exist

cases when even in the limit of long measurement times an inequality holds [12,13]

$$\lim_{T\to\infty} \overline{\delta^2(\Delta)} \neq \langle \mathbf{r}^2(\Delta) \rangle. \tag{9}$$

This is the situation when the process violates the Boltzmann–Khinchin ergodic hypothesis [72]. In fact in living biological cells as well as in in vivo experiments such non-ergodic behaviour was explicitly measured, see the reviews [9,12–14]. In the above listed systems the non-ergodic behaviour was identified in several cases [52,53,59], and we will see further examples in the study of membrane systems below. Non-ergodicity of the form Eq. (9) is commonly due to the non-stationarity of the associated process [13,14].

Non-ergodic behaviour can be accompanied by an intrinsic irreproducibility of time averaged quantities in the sense that repeated measurements show a pronounced spread of the time averaged observable [12,13,73,74]. For the time averaged mean squared displacement this spread is quantified in terms of the dimensionless variable

$$\xi(\Delta) = \frac{\overline{\delta^2(\Delta)}}{\left\langle \overline{\delta^2(\Delta)} \right\rangle}. \tag{10}$$

Based on this quantity we can determine the distribution function $\phi(\xi)$ around the ergodic value $\xi = 1$ which is a good indicator for the underlying stochastic process [12,13,75,76]. This spread is often also expressed in terms of the variance of the function ϕ, the so-called ergodicity breaking parameter [13,75,77]

$$\text{EB}(\Delta) = \left\langle \xi^2(\Delta) \right\rangle - \langle \xi(\Delta) \rangle^2 = \left\langle \xi^2(\Delta) \right\rangle - 1. \tag{11}$$

For a given lag time is describes the deviation of the system from the ergodic behaviour. For finite measurement times even standard Brownian motion is not perfectly ergodic, however in the limit of short lag times or long trajectories the ergodicity breaking parameter converges to zero as [78]

$$\lim_{\Delta/T\to0} \text{EB}_{\text{BM}}(\Delta) = \frac{4\Delta}{3T}. \tag{12}$$

In other systems, the asymptotic value of EB for small values of Δ/T may remain finite, see below. The parameters $\text{EB}(\Delta)$ and $G(\Delta)$, involving higher moments of the particle displacement, are known to be sensitive indicators of the type of the anomalous diffusion process [13,19,79].

Finally, we mention that for non-stationary processes significant *ageing* of the system may be observed. Thus, the effective diffusivity of a subdiffusive system may become a decaying function of time [12,13, 52,53]. In other words the measurement of the system will produce different information when we start it at different times after the original preparation of the system. Such a behaviour is well known from glassy systems [80,81], for which the term *ageing* was originally coined. In ageing systems the time averaged mean squared displacement then becomes a function of the ageing time t_a, from which we evaluate the time series of the particle displacement [13,82]

$$\overline{\delta_a^2(\Delta)} = \frac{1}{T-\Delta} \int_{t_a}^{T+t_a-\Delta} (\mathbf{r}(t+\Delta) - \mathbf{r}(t))^2 \, dt. \tag{13}$$

4. In vivo anomalous diffusion in membranes

According to the model developed by Saffmann and Delbrück in 1975 the components of biological membranes perform Brownian motion [83]. Using FCS measurements, however, *anomalous diffusion* of different dye molecules in membranes was reported by Schwille et al. [45]. A detailed study comparing FCS data of fluorescently tagged enzymes in the membranes of the endoplasmatic reticulum and the Golgi apparatus in HeLa cells with simulations of anomalous diffusion processes was then presented by Weiss et al. [84]. Using the possibilities of superresolution microscopy Weigel et al. managed to monitor the motion of single channel proteins embedded in the plasma membrane of living kidney cells over minute time ranges [85], as shown in Fig. 4.

Following the theoretical discussion of non-ergodic motion in anomalous diffusion processes in Refs. [75,86] and the identification of such motion in the cytoplasm of living yeast cells [52], Weigel et al. reported a similar behaviour in the plasma membrane. In the recorded trajectories one can see that the channel protein moves quite vividly for a certain period of time until its motion becomes replaced by a localised rattling. Only after a waiting period τ the channel protein resumes its motion, until it is *trapped* again [85]. The statistics of the waiting periods exhibits an asymptotic power-law scaling of the form

$$\psi(\tau) \simeq \tau^{-1-\alpha} \tag{14}$$

with the scaling exponent $\alpha \approx 0.9$, as demonstrated in Fig. 5 [85]. In the analysis of their data the authors also found that the motion of the protein channels shows *ageing* behaviour in the form of the dependence of the observed value of the time averaged mean squared displacement Eq. (5) on the measurement time [85]; see also Fig. 5. In the course of time, that is, the channels become less and less mobile. As studied in more detail in Ref. [87] this, on first sight strange behaviour may be related to the physiological function of the specific protein channels under observation.

In fact this behaviour is not that strange. Consider the distribution of waiting times (Eq. (14)) and combine this with the general framework of the Scher–Montroll continuous time random walk model such that the walker may perform a jump after a random waiting time drawn from $\psi(\tau)$ [88]. It is easy to see that the characteristic waiting time $\langle \tau \rangle =$
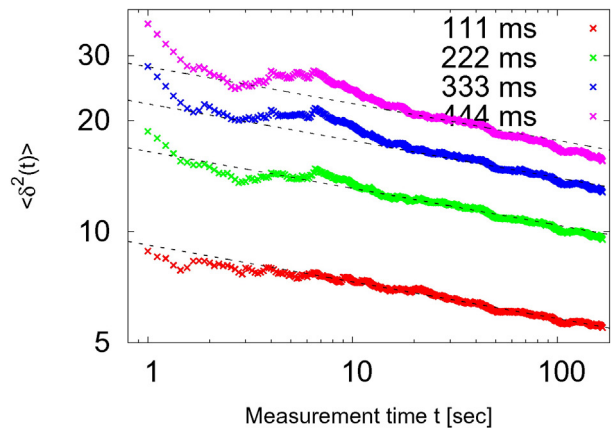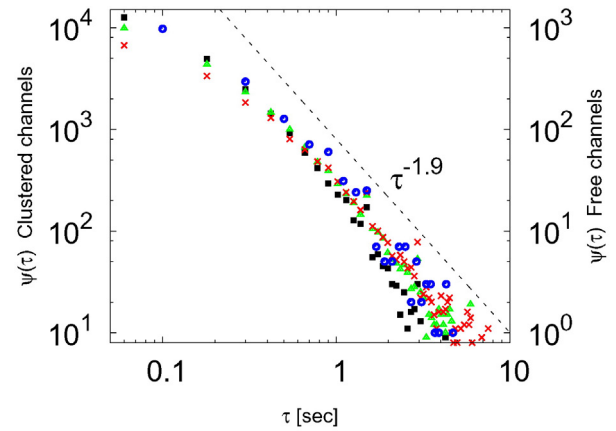
Fig. 5. Distribution of immobilisation (waiting) times (top) and ageing behaviour of the time averaged mean squared displacement (bottom) for the motion of protein channels in the plasma membrane of living eukaryotic cells [85]. Data courtesy D. Krapf.

$\int_{\tau^*}^{\infty} \tau' \psi(\tau') d\tau'$, with some microscopic lower cutoff τ^*, will diverge for $0 < \alpha < 1$. Thus, there is no longer a characteristic time scale allowing us to separate between a single or few jump events and many jumps, and the very notion of a long time limit ceases to exist. For such processes it was shown that while the ensemble averaged mean squared displacement follows the power-law scaling (Eq. (3)) with $\beta = \alpha$, the trajectory-averaged time averaged mean squared displacement shows a *linear* scaling

$$\left\langle \overline{\delta^2(\Delta)} \right\rangle \simeq K_\beta \frac{\Delta}{T^{1-\beta}} \tag{15}$$

with the lag time Δ [12,13,75,86]. This non-ergodic behaviour is also characteristic for other non-stationary processes such as Markovian diffusion with space or time dependent diffusion coefficients [89–93]. We also recognise the explicit dependence on the measurement time T in Eq. (15), which is seen in Fig. 5. We note that subdiffusive continuous time random walks were also proposed to capture the observed dynamics in glassy systems [94].

Similar results with regards to the scaling of the mean squared displacement and the ageing behaviour were reported by Manzo et al. for the motion of DC-SIGN receptor protein and its mutants [95], as reported in Fig. 6. Again, the non-ergodic and ageing behaviour is observed, along with a broad distribution of the diffusivity characteristic for non-ergodic processes [12,13,75,76].

The potential causes for the anomalous diffusion behaviour of embedded proteins in cellular membranes are related to the crowding of the lipid membrane itself, an extreme example of which is shown in Fig. 1. Indeed, the cellular plasma membrane is a highly crowded
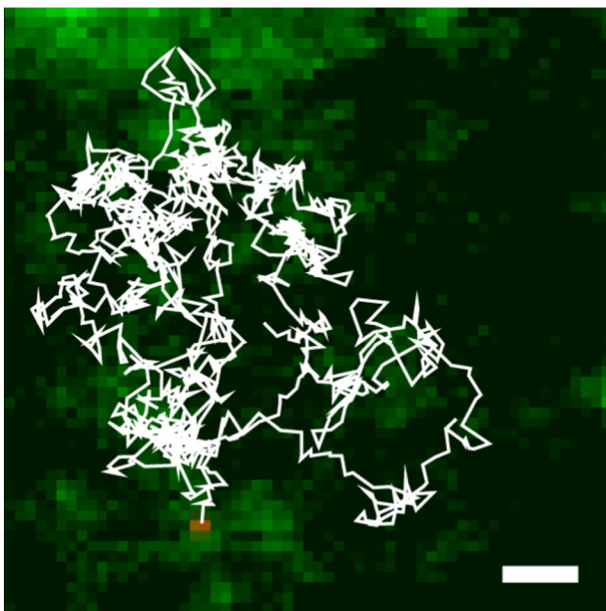

Fig. 4. Trace of a labelled voltage-gated Kv2.1 potassium channel protein on a plasma membrane of a living human embryotic kidney cell [85]. The scale bar is 1 μm. Figure courtesy D. Krapf, Colorado State University, Fort Collins.
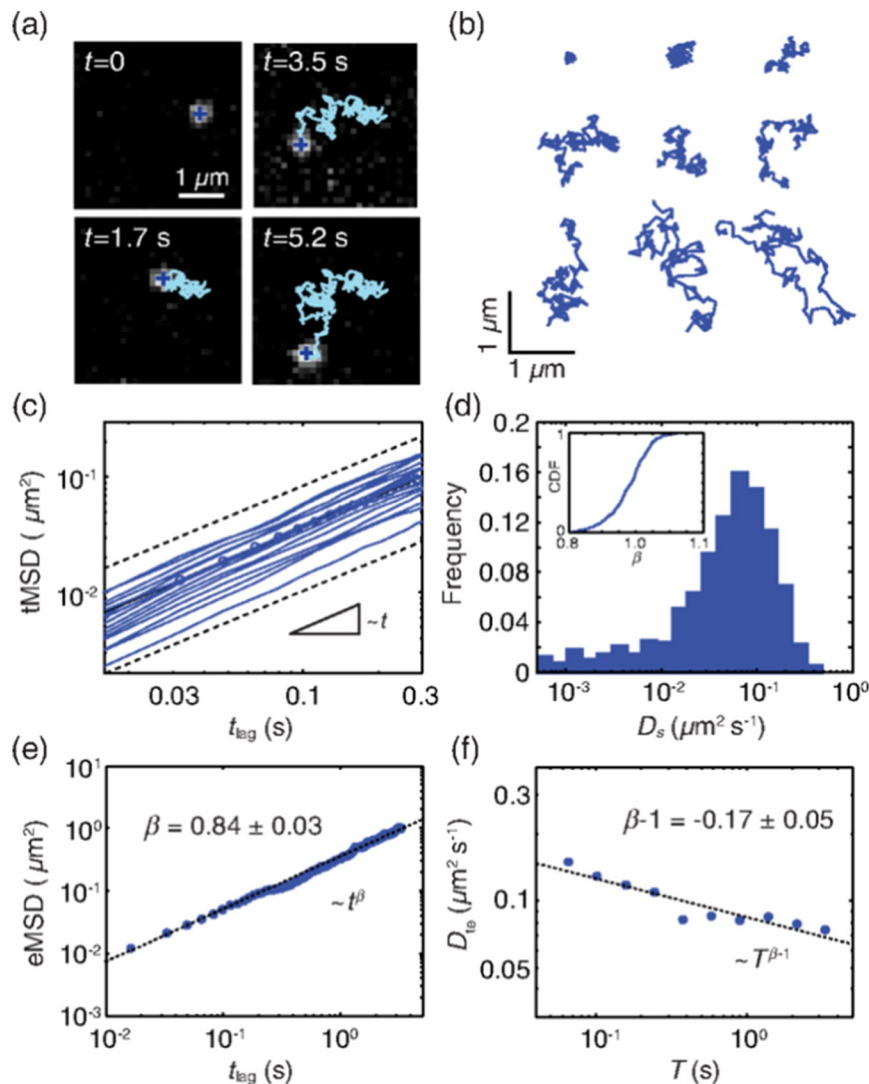
Fig. 6. DC-SIGN diffusion shows non-ergodicity and ageing. (a) Time traces of quantum-dot-labelled DC-SIGN nonintegrin proteins diffusing on the dorsal membrane of a Chinese hamster ovary cell. (b) Representative trajectories for identical recording time $T = 3.2$ s. (c) Log–log plot of the time averaged mean squared displacement for individual trajectories (blue lines). The dashed lines indicate the linear scaling in time. The circles correspond to the average $\langle \overline{\delta^2(\Delta)} \rangle$. (d) Distribution of the short time diffusion coefficients for all trajectories. Inset: Cumulative distribution function of the scaling exponent β. (e) Log–log plot of the ensemble-averaged mean squared displacement $\langle \mathbf{r}^2(t) \rangle$. A fit of the data (dashed line) provides the exponent $\beta = 0.84$, showing subdiffusion. (f) Log–log plot of the diffusion coefficient as a function of the observation time T, corresponding to the ageing dependence in Eq. (15). The fitted slope $1 - \beta = 0.17$ is in good agreement with the value of β found in panel (e) [95].

interface with up to 25% of the total area [96] occupied by various membrane proteins, ion channels, and pores [85,97]; see Fig. 1. These enable the communication of cells with the environment and active exchange of chemicals and other products [98]. However, as discussed in Refs. [85,87,95], the contact to the inside of the cell, in particular, the mechanical elements of the cytoskeleton, provide an additional complication of the motion. An interesting phenomenon is also the dynamics of bulk mediated surface diffusion in which biomolecules such as proteins intermittently bind to the membrane surface and undergo transient excursions into the adjacent bulk volume. This phenomenon was just quantified experimentally [99] and shown to be consistent with the analytically predicted behaviour [100].

From the results reported here, we conclude that the motion of embedded, larger entities such as channel proteins in membranes is subdiffusive over time ranges of some 10 ms to 100 s as measured by single particle tracking [85,95], and some 10 μs to 1 s by FCS measurements [84]. Insight into shorter time dynamics and on a resolution of single lipids is provided by simulations, albeit the first step towards experimental observation of such motion is provided by novel stimulated emission depletion microscopy (STED) techniques [101], by which

indeed anomalous diffusion of lipids could be observed [102]. Otherwise, methods such as neutron scattering needs to be employed to resolved the short time behaviour of lipid molecules [103]. We note that a recent overview of the advances and experimental as well as simulations methods to examine non-Brownian lipid and protein diffusion in crowded membranes is also provided in Ref. [104].

5. Anomalous membrane diffusion in silico

We now review the anomalous diffusion of lipid molecules and crowders such as cholesterol or proteins in lipid bilayer membranes observed in massive computer simulations.

5.1. Pure lipid bilayer systems

Lipid bilayers are effectively two-dimensional systems, which are highly packed with phospholipid molecules, which undergo thermally driven lateral diffusion and thus constantly reorganise the membrane. The dynamic behaviour of such lipid bilayer systems has been extensively studied in terms of molecular dynamics simulations using both

all atom and coarse grained approaches. Generally, the lateral mean squared displacement in such simulations spans three distinct regimes: (i) a short time ballistic growth with $\alpha = 2$ due to inertial effects, followed by (ii) a subdiffusive regime with $0 < \alpha < 1$ at intermediate time, and (iii) a normal diffusive long time regime [105]. The long time regime has been studied extensively for a range of phospholipid molecules, see, for instance, Refs. [106]. As we will discuss, lipid diffusion in pure bilayers occurs both in the liquid phases and in the gel phase below the melting temperature, the latter with decreased diffusivity. Moreover, in bilayers mixed with cholesterols, the lipid mobility decreases with higher cholesterol concentration, as discussed in the next subsection.

The intermediate time range subdiffusion of lipid molecules is relatively poorly understood. The traditional microscopic picture claims that the lateral motion of the lipid molecules occurs via more or less sudden jumps upon availability of sufficient thermally activated void space at nearest sites [108–110]. In between successive jumps the lipid molecule is being caged by its neighbours and undergoes a rattling-like motion. This jump-diffusion model in the spirit of a continuous time random walk was used to estimate the lipid diffusivities in the liquid-disordered phase and in cholesterol containing bilayers [107,108]. However, extensive atomistic molecular dynamics simulations [111] as well as quasi-elastic neutron scattering experiments [112] demonstrated that such jump-like displacements rarely occur. Rather the lipid molecules move in a concerted fashion, correlated with their neighbours as loose clusters.

Can we learn more about the fundamental physical nature of the lipid motion in pure lipid bilayers from the exact stochastic behaviour of the lipids in simulations? Ref. [105] shows that the lipid motion is approximately Gaussian at time scales above some 10 ns, albeit significant non-Gaussianity occurs for the lateral motion at shorter time scales. A more detailed analysis from a stochastic point of view is provided by Kneller et al. [113], further detailed in Ref. [114], compare also Ref. [115]. From the velocity correlation function the authors concluded that the lipid motion is described best by the fractional Langevin equation [13,113,116–118]

$$m\frac{d^2x(t)}{dt^2} = -\gamma^* \int_0^t (t-t')^{\alpha-2}\left(\frac{dx(t')}{dt'}\right)dt' + \eta^*\xi_{fGn}(t), \qquad (16)$$

where γ^* is a friction coefficient of physical dimension $[\gamma^*] = g \times s^{-\alpha}$ and $\xi_{fGn}(t)$ represents the fractional Gaussian noise with power-law correlation

$$\langle \xi_{fGn}(t_1)\xi_{fGn}(t_2)\rangle = \alpha(\alpha-1)K_\alpha^*|t_1-t_2|^{\alpha-2} \qquad (17)$$

for $t_1, t_2 > 0$ and $t_1 \neq t_2$, with $1 < \alpha < 2$ such that the fluctuation dissipation relation is fulfilled [117–120]. Here the coefficients η^* and K_α^* are coupled by the fluctuation–dissipation relation $\eta^* = \sqrt{\gamma^* k_B T / [K_\alpha^* \alpha(\alpha-1)]}$ [13]. The dynamic Eq. (16) exhibits a slowly decaying power-law memory (on the level of the stochastic equation) [13,113,118]. An alternative stochastic interpretation of the lipid motion was given in Ref. [121], in which jump-like continuous time random walk motion governed by non-Gaussian fluctuations and scale-free rattling dynamics were proposed based on an analysis of the trapping time distributions and the mean maximal excursion method [17]. As we discuss now, the detailed analysis provided in Ref. [71] turns out in support of the Gaussian, fractional Langevin equation motion picture.

Fig. 8 shows the trajectory-mean $\langle \overline{\delta^2(\Delta)}\rangle$ of the time averaged mean squared displacement including the trajectories of all phospholipids. All three lipid chemistries 1,2-Distearoyl-sn-glycero-3-phosphocholine (DSPC), 1-stearoyl-2-oleoyl-sn-glycero-3-phosphocholine (SOPC), and 1,2-Dioleoyl-sn-glycero-3-phosphocholine (DOPC) are analysed in the liquid disordered phase. Panel A depicts the lipid diffusion for pure single chemistry lipid bilayers, whereas Panel B represents the data for bilayers with added cholesterol, see the next subsection. In all cases the resulting curves were fitted by a power-law $\langle \overline{\delta^2(\Delta)}\rangle = 4K_\alpha \Delta^\alpha$, separately at short and long times. The corresponding anomalous diffusion exponents α are indicated in the Panels. Accordingly, in the pure lipid bilayers all three chemistries of lipid molecules show analogous behaviour. Namely, we observe anomalous diffusion with a scaling exponent $\alpha \sim 0.6$ below a crossover time of $\tau_c \sim 10$ ns. Beyond that time the lipid molecules exhibit approximately normal Brownian motion. This crossover time τ_c corresponds roughly to the diffusion time that a single lipid molecule needs to move over a distance corresponding to the nearest-neighbour separation. The differences in the tail structure between these lipids affect slightly the lipid diffusivity [71].

To analyse these claims deeper in Ref. [71] we performed molecular dynamics simulations of lipid bilayers of 128 phospholipid molecules in the liquid disordered phase. Three pure single component bilayers composed of the lipid chemistries DSPC, SOPC, and DOPC phospholipids were employed. To avoid spurious dynamics due to the free, independent translational motion of the upper and lower lipid layers, we analyse the relative motion $\mathbf{r}(t)$ of the lipids with respect to the centre of mass of the lipids. Fig. 7 shows a snapshot of the simulated lipids along with the water layer.

Fig. 9 shows the analysis of the obtained single lipid molecule traces. The individual traces are ergodic and do not exhibit ageing (Fig. 9B), and the amplitude scatter follows a relatively narrow bell shape. Together with the moment ratios we find a clear result in favour of the Gaussian
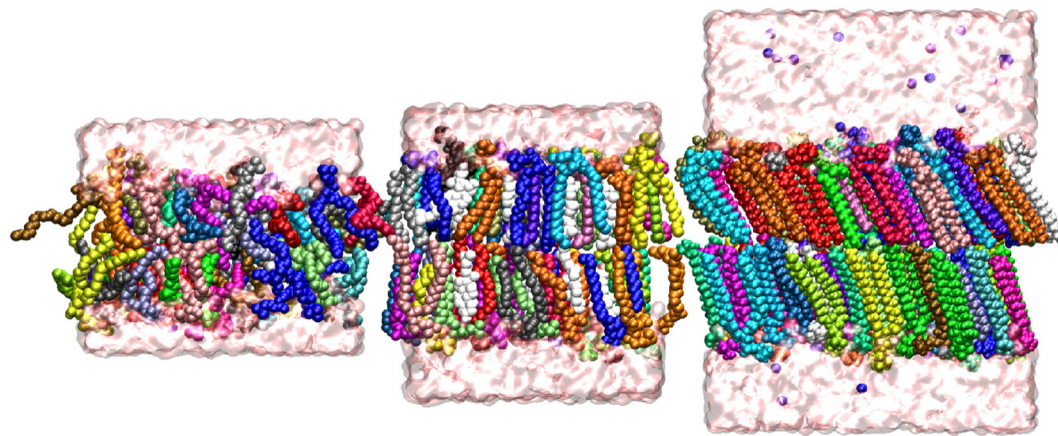

Fig. 7. Snapshots of the lipid bilayer consisting of DOPC at 338 K (left), a mixture of DSPC and cholesterols at 338 K (middle), and DSPC at 310 K (right). These systems correspond to the liquid disordered, liquid ordered, and gel phases, respectively. Each lipid is rendered in a different colour. Explicit water molecules are represented by the upper and lower transparent layers. Cholesterols appear in white (middle), Na $^+$ and Cl $^-$ ions as blue spheres (right) [71].

anomalous diffusion picture. Finally, the displacement correlator

$$C_{\delta t}(t) = \frac{1}{\delta t^2} \langle [\mathbf{r}(t + \delta t) - \mathbf{r}(t)] \times [\mathbf{r}(\delta t) - \mathbf{r}(0)] \rangle \qquad (18)$$

for a given time step δt can be shown to have a fit free normalised shape $C_{\delta t}(t)/C_{\delta t}(0)$ for any given values of δt and α [71]. The result shown in Fig. 9D for $C_{\delta t}(t)/C_{\delta t}(0)$ is fully consistent with those results obtained in Ref. [113], supporting the fact that the fractional Langevin Eq. (16) governs the lipid motion [71]. We stress that this form for the velocity autocorrelation function cannot be consistent with a continuous time random walks picture for the periodic boundary conditions used here [72], compare Fig. 9D. Moreover, we demonstrated that the rattling motion and the escape of a lipid molecule from a finite area are both consistent with the Gaussian anomalous diffusion picture [71]. Moreover, a further analysis [71] demonstrates that the motion is consistent with the observation of the collective motion of lipids in flow-like patterns, as originally reported in Refs. [111,112].

We note that membrane hydration water in fluid-phase lipid bilayers also exhibits anomalous diffusion, as studied by computer simulations and quasi-elastic neutron scattering in Refs. [122,123], see also Ref. [216]. In these studies the physical origins, such as caging effects in the membrane-associated water, are also discussed. Similarly the diffusion of protons on lipid membranes is anomalous [124].

5.2. Lipid membranes with cholesterol and gel phase dynamics

Cholesterol is a lipid molecule, which is biosynthesised by all animal cells. Cholesterol is an integral structural component of the cell membranes necessary for the mechanical membrane structural integrity while allowing it to remain fluid. In contrast to plant cells and bacteria animal cells therefore do not need a cell wall and are often able to move about. Cholesterol is known to tune lipid–lipid interaction potentials often leading to aggregation [125] and supramolecular complex formation [126]. This in turn controls the protein preference for liquid ordered versus disordered lipid phases [127] by cooperative action [128,129]. A certain demixing of lipid components, dynamical composition heterogeneities, and pattern formation [130] can be the prerequisite for a proper functioning of membrane-associated proteins, often orchestrated by lipid–protein interactions [98,131,132]. The latter include both close range contacts and membrane mediated forces of a longer range [133], see also the next section.

To study how the presence of cholesterol changes the quality of the lipid diffusion in our model system, we investigated the lipid bilayer dynamics for three different lipid chemistries with additional 32 cholesterols (20% molar concentration). The resulting organisation and structure of the combined lipid–cholesterol bilayer corresponds to the liquid ordered phase, as shown in Fig. 7 in the middle panel. The existence of such a liquid ordered phase was confirmed by neutron spin-echo and neutron backscattering, revealing ordered lipid domains of a size of some 220 Å [134]. This result is consistent with the coarse grained simulations presented in Ref. [135], see also Ref. [136].

Fig. 8B shows the time averaged mean squared displacement for cholesterol-containing bilayers. Interestingly, the presence of the cholesterols significantly alters both the short and the long time lipid diffusion. The most significant difference occurs for the saturated DSPC molecules with the smallest lipid cross section area [137]. We observe that below the crossover time, which again is of the order of $\tau_c \approx 10$ ns, the anomalous diffusion exponent α decreases to about 0.5. More importantly, a new subdiffusion regime emerges with $\alpha \sim 0.8$ which lasts up to 100 ns. An additional simulation of 1 µs length confirms that this new long time regime is actually a slow transition towards normal diffusion that, however, lasts over hundreds of nanoseconds. In the time window shown in Fig. 8 the diffusion is well fitted by power-laws. For the unsaturated DOPC molecules, the effect of the added cholesterols is small, mostly affecting the lipid diffusivity but not the anomalous scaling exponent. In particular, no subdiffusion is observed beyond the crossover time τ_c [71].

Analysing the dynamics of the cholesterol-containing bilayer further, the ergodic nature of the diffusion patterns of both the lipid molecules and the cholesterols is preserved [71]. Concurrently, the presence of the cholesterols markedly affects the amplitude variation of individual time traces, as captured in the distribution $\phi(\xi)$. Namely, compared to the case of the pure bilayer shown in Panel C of Fig. 9, when cholesterols are added $\phi(\xi)$ becomes significantly broader, as shown in Fig. 10B. This observation underlines the fact that individual lipids undergo considerable variations in their local mobility in the presence of cholesterols, as indeed observed in Panel A of Fig. 10 [71]. This observation is consistent with the above mentioned findings of heterogeneously structured membranes [134,135]. We also note that with cholesterols the displacement correlation function $C_{\delta t}(t)$ assumes a somewhat deeper well reflecting a stronger anti-correlation in the molecular motion [71].

When we follow the motion of the cholesterols themselves and analyse their stochastic behaviour we observe that, in full analogy to
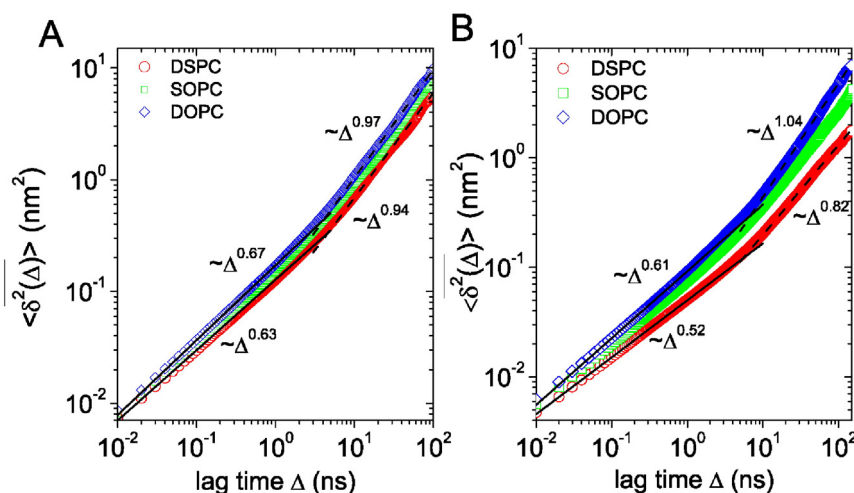

Fig. 8. Time averaged mean squared displacements $\overline{\langle \delta^2(\Delta) \rangle}$, which are further averaged over the trajectories of all 128 lipid molecules in the model membrane sheet of single lipid chemistry bilayers in the liquid disordered phases of DSPC, SOPC, and DOPC lipids. A: Cholesterol-free case. B: With cholesterol. The scaling exponents for both the short and long lag time behaviour are indicated in the Panels. Pure lipid bilayers perform approximately Brownian diffusion beyond 10 ns, while cholesterol-containing bilayers in the DSPC case show a prolonged subdiffusion [71].
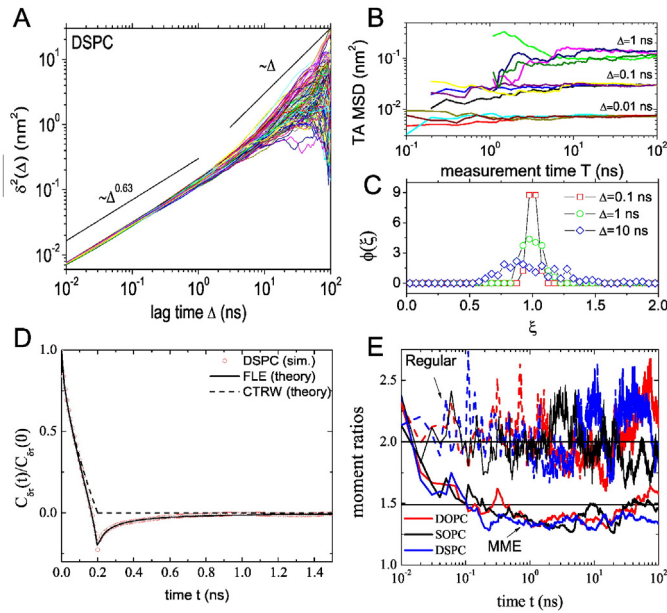
Fig. 9. Analysis of the DSPC motion in a pure liquid phase bilayer. A. Time averaged mean squared displacement $\overline{\delta^2(\Delta)}$ of all 128 DSPC molecules. B. $\overline{\delta^2(\Delta)}$ as function of the measurement time T, for lag times $\Delta = 0.01$, 0.1, 1 ns. C. Normalised amplitude scatter distribution $\phi(\xi)$ of $\overline{\delta^2(\Delta)}$ versus $\xi = \overline{\delta^2(\Delta)}/\langle\overline{\delta^2(\Delta)}\rangle$, for $\Delta = 0.1$, 1, 10 ns. D. Displacement autocorrelation function $C_{\delta t}(t)/C_{\delta t}(0)$ of DSPC lipids, $\delta t = 0.2$ ns. The solid and dotted lines represent the fit-free forms of $C_{\delta t}(t)/C_{\delta t}(0)$ for the fractional Langevin equation and the continuous time random walk at $\alpha = 0.63$. E. Moment ratios $\langle \mathbf{r}^4(t)\rangle / \langle \mathbf{r}^2(t)\rangle^2$ (regular) and $\langle r_{\max}^4(t)\rangle / \langle r_{\max}^2(t)\rangle^2$ [mean maximal excursion (MME)] for DSPC, SOPC, and DOPC molecules. The horizontal line at 1.49 distinguishes fractional Langevin equation motion ($\langle r_{\max}^4(t)\rangle / \langle r_{\max}^2(t)\rangle^2 < 1.49$) from continuous time random walks ($\langle r_{\max}^4(t)\rangle / \langle r_{\max}^2(t)\rangle^2 > 1.49$). The horizontal line at 2 is the expected value of the regular moment ratio for both types of motion [71].

the lipid molecules, their diffusive motion corresponds to the fractional Langevin equation picture already identified for the lipids. As we demonstrate in Panel A of Fig. 10 the cholesterols have a somewhat higher diffusivity compared to the lipids, the associated anomalous diffusion exponents of both species are essentially identical. However, the analysis shows that the amplitude scatter distribution of the cholesterols are somewhat more concentrated around the ergodic value $\xi = 1$, supporting that the motion of the cholesterols is more uniform than the motion of the lipids. Also the displacement correlation function and the moment ratios are hardly different between lipids and cholesterols [71].

Let us finally address the case of the third known state of pure lipid bilayers, namely, the gel phase shown in the right panel of Fig. 7. All

Fig. 10. Mixture of DSPC lipid molecules in a liquid phase bilayer membrane with cholesterol molecules. A: single trace time averaged mean squared displacements $\overline{\delta^2(\Delta)}$ for all 128 DSPC molecules. The mean, trajectory averages of $\overline{\delta^2(\Delta)}$ are shown for both the DSPC lipids (red squares) and the cholesterols (blue circle). For clarity, these two curves were shifted up by a factor of 20. B: Amplitude scatter distribution $\phi(\xi)$ of the time averaged mean squared displacements of DSPCs and cholesterols [71].

lipids have a characteristic phase transition temperature at which they pass from the ('solid') gel phase to the so-far considered liquid phase [138]. In the gel phase the lipids are still able to exchange positions with their neighbours and in that sense have a liquid-like character, yet their mobility is significantly decreased. As can be seen from Fig. 7 the tails of the individual lipids are almost fully devoid of internal fluctuations, causing the width of the bilayer to increase. Does this significant change in the conformation space of the lipids affect the stochastic nature of their motion?

For a bilayer composed of DSPC lipid molecules Panel A of Fig. 11 demonstrates that the diffusion described by the time averaged mean squared displacement $\langle\overline{\delta^2}\rangle$ exhibits an extremely small anomalous diffusion exponent $\alpha \approx 0.16$ at short times. It is significantly smaller than the value found for the liquid phase of $\alpha \approx 0.6$. In addition to this, we observe a more prolonged subdiffusion with $\alpha \approx 0.59$ beyond the crossover time, which remains of the order $\tau_c \approx 10$ ns. As shown in Panel B of Fig. 11 the recorded lipid motion in the gel phase is fully consistent with the fractional Langevin equation description, here demonstrated for the excellent match between the theoretical displacement correlation function and the analysed data. We note that both the amplitude variation between individual time traces $\overline{\delta^2(\Delta)}$ and the moment ratios provide further support for the ergodic, fractional Langevin equation driven motion [71].

We note that for multi-component membranes additional important effects occur such as a fluid–gel phase coexistence [139]. Moreover, near-critical fluctuations were studied recently by coarse-grained simulations, revealing anomalous diffusion of the lipids near the coexistence point [140].

5.3. Diffusion in protein crowded lipid bilayers

The pure lipid and cholesterol-containing bilayer membrane systems discussed so far are idealised model systems designed to study fundamental physical properties. In the lab these systems can indeed be synthesised and analysed by various experimental tools, such as the above-mentioned neutron scattering, fluorescence correlation, or optical microscopy methods [104]. Biologically relevant membranes, however, contain by necessity channels or receptors to allow for the exchange of material or molecular information between the two volumes separated by the membrane surface. While in Fig. 1 we show an extreme case of crowding, simulations now are able to capture relevant degrees of crowding in which the model membranes are decorated with a range of different membrane proteins, as depicted in Fig. 12. In general, the physical setting of crowded membranes combines membrane constituent particles of markedly different size and molecular mass.

As for the numbers, it was suggested that the molar (number) ratio of embedded proteins and lipid molecules varies between some 1:50 and 1:100 [96,142]. Practically this means that if we take the typical cross section area of 0.64 nm^2 of a phospholipid and compare it with a typical α-helical transmembrane protein with 3 nm diameter, for a protein–lipid of 1:50 we typically find that the distance between the surfaces of vicinal proteins is as small as 3.2 nm. This number suggests that in lipid membranes, that are crowded with proteins, interactions between proteins may play a decisive role in the lateral diffusion behaviour in the membrane. In particular it becomes a major question in how far the presence of the proteins affects the very diffusion behaviour of the smaller lipid molecules.

As discussed in Section 4 experiments showed that in the membranes of living cells the diffusive behaviour of both proteins and lipids is significantly different in comparison to simplified model systems [84,85,101,143–146]. A particular striking observation is that the diffusivities of individual proteins in different regions of a cellular membrane vary up to five-fold, even when the protein motion is recorded up to macroscopic time scales [144]. Concurrently, the diffusion of the very lipids may also exhibit complex features. Namely, super-
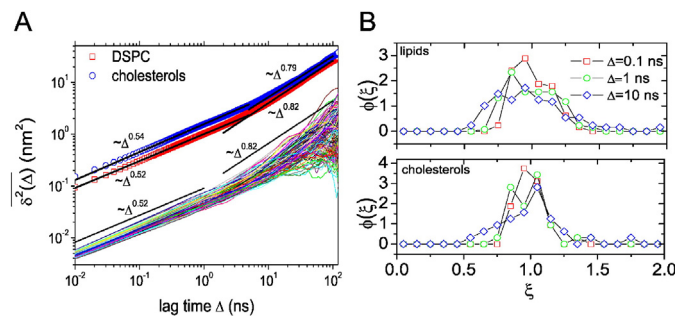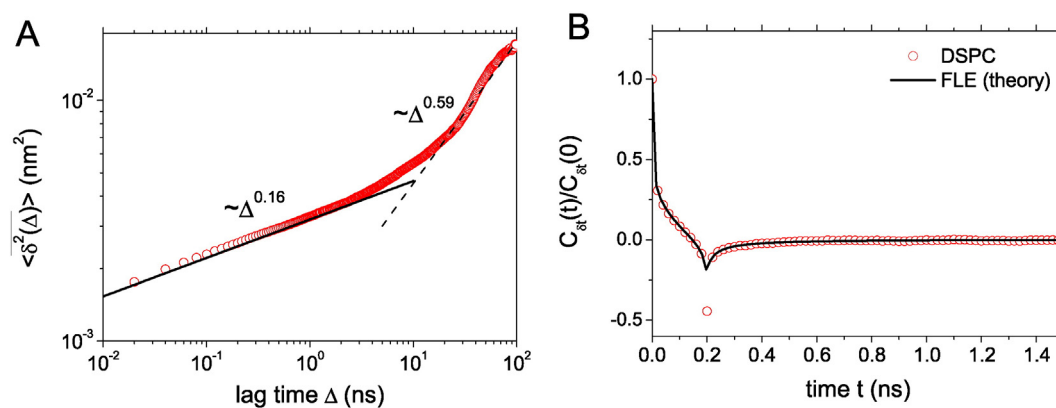
Fig. 11. Lipid diffusion in the gel phase of a bilayer of DSPC lipid molecules. A: Time averaged mean squared displacement $\overline{\langle \delta^2(\Delta) \rangle}$ over all lipid trajectories. B: Displacement autocorrelation function $C_{\delta t}(t)/C_{\delta t}(0)$ with time step $\delta t = 0.2$ ns. The solid line shows the (fit-free) theoretical result for the fractional Langevin equation with $\alpha = 0.16$ [71].

resolution microscopy imaging in living biological cells showed that the mobility of the lipids may be reduced significantly on the millisecond time range corresponding to length scales of some tens of nm [101], suggesting that there are exist mechanisms confining specific lipid types (see also Ref. [147]).

To better understand the consequences to the motion of both proteins and lipids in crowded membrane bilayer systems coarse grained models were simulated [148]. The membranes were made up of dilinoleoylphosphatidylcholine (DLPC) and dipalmitoylphosphatidylcholine (DPPC) lipids, respectively, with a varying number of embedded NaK channel (2AHY) proteins. The lipids in conjunction with the protein channel were chosen such that for the DLPC bilayers the NaK channels do not aggregate due to the minor protein–lipid hydrophobic mismatch. In contrast, in the DPPC bilayers the hydrophobic mismatch is larger and NaK channels prefer forming aggregates [148]. Both systems were studied for multiple protein–lipid ratios. Snapshots of both cases are shown in Fig. 13.

In the simulations proteins in the aggregating systems start to form aggregates as early as after a few hundred nanoseconds. Almost all of the proteins become connected during the first microsecond. The protein clusters are quite stable. In contrast, in the non-aggregating systems the proteins tend to stay apart from each other for up to microseconds, some of them even for the entire simulated 10 μs. Aggregates, that do form, are transient and rapidly break apart again. These different tendencies towards aggregate formation are not caused by the lateral mobilities. In the non-aggregating membrane the proteins are found to have a higher mobility than in the aggregating systems. The proteins

therefore are able to meet each other more rapidly, yet in the slower aggregating system any aggregates form faster [148].

Let us start our diffusion analysis with the long time diffusion coefficient, obtained from the approximately normal diffusive regimes, formally

$$K_1 = \lim_{t \to \infty} \frac{\langle \mathbf{r}^2(t) \rangle}{4t}. \tag{19}$$

From the plots of the long time diffusion coefficients in Fig. 14 we see that in the dilute case the lipid diffusion is considerably faster in the non-aggregating case, reflecting the properties of the DLPC versus the DPPC bilayer. Simultaneously, albeit somewhat less pronounced, the single embedded protein tracer in the non-aggregating bilayer is more mobile. The lipid diffusivity then systematically decreases with increasing protein crowding. The decrease is approximately linear, and from the dilute to the crowded case (1:50 protein:lipid ratio) the decrease corresponds to a fivefold reduction for the non-aggregating system. In the aggregating case the decrease is more pronounced, given by a factor ≈20, see the red data points in Fig. 14. For the lipids Fig. 14 also shows that the motion in x and y directions is approximately the same, as it should be.

The shape of the curve relating the protein diffusivity to the protein:lipid ratio differs significantly and exhibits a distinct kink between the ratio 1:150 and 1:100. In the non-aggregating system the overall drop from the dilute to the 1:50 crowded case is ≈25 fold, for the aggregating case the corresponding factor is around 100 [148]. In
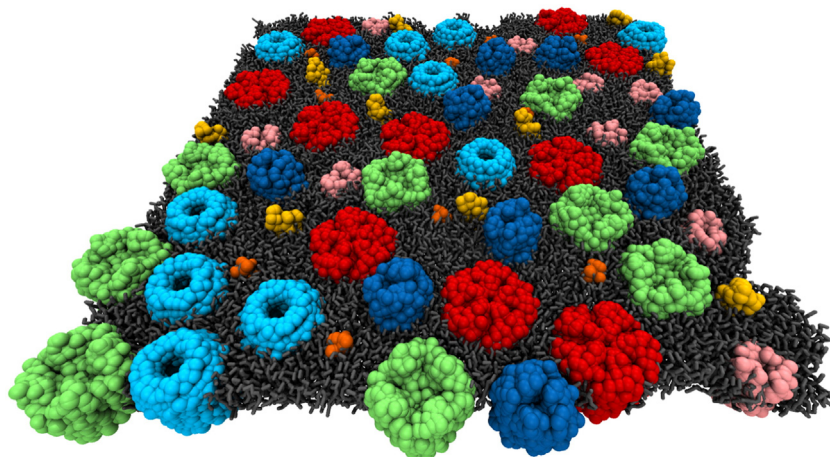

Fig. 12. Crowded model membrane containing a mix of protein types of varying shape and size. Figure courtesy M. Javanainen.
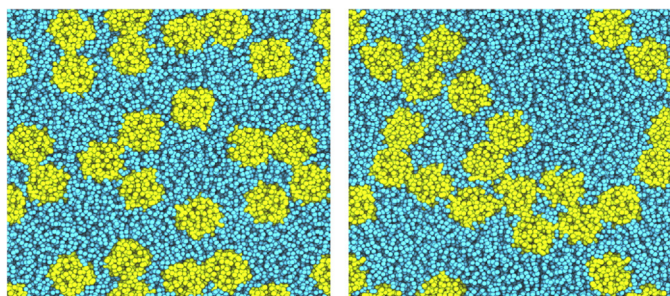
Fig. 13. Protein crowded lipid bilayer membrane in absence (left) and presence (right) of protein aggregates. Figures courtesy Matti Javanainen.

particular, in the most crowded aggregating system the protein motion has virtually stopped, the diffusivity is down to $\approx 4 \times 10^{-10}$ cm^2/s. Comparing the diffusivities of lipids and proteins the diffusion of proteins is slower by a factor of 5 (protein-poor) to 30 (protein-rich conditions), compare Fig. 14.

The diffusion of both lipids and proteins is anomalous in the membrane. This is demonstrated in Fig. 15 depicting the time dependent anomalous diffusion exponent $\alpha(t)$ determined from the local slope of $\langle \mathbf{r}^2(t) \rangle$ in a log–log plot. In Fig. 15 we show the scaling exponent $\alpha(t)$ for the lipids in the non-aggregating and aggregating cases, the corresponding results for the proteins are shown in Fig. 16. We first note that in the dilute case the shape of $\alpha(t)$ is almost identical for both the non-aggregating and aggregating systems. Any differences between the two systems in the crowded case are therefore not due to a different dynamics of the lipid molecules but are consequences of the different aggregation behaviour of the proteins.

Let us now focus on the lipid motion. In the non-aggregating systems we observe that generally the variation of $\alpha(t)$ is less pronounced than in the aggregating case, in particular the observed dip at around 1 µs is much less pronounced. Instead, we observe an approximate plateau over the range of an order of magnitude in time, from a few tens of nanoseconds to a few hundred nanoseconds. The plateau appears as a common feature in all non-aggregating systems. Seen for varying protein crowding we find a systematic decease of the scaling exponent with growing crowding fraction, in agreement with experiments [149]. In the dilute case normal diffusion is eventually recovered at around 100 ns, when more proteins are added this onset of Brownian motion is markedly shifted to longer times. Even for the case of lesser crowding with 1:200 for the protein:lipid ratio we see that this onset is already shifted to some 1 µs. With increasing crowding it becomes more

ambiguous to extract the crossover time to normal diffusion, based on rough estimated the time scale is on the range of 10 to 100 µs [148].

For the aggregating case we observe that the crossover to Brownian motion occurs somewhat later than in the non-aggregating case. Distinct is especially the stark decrease of the value of $\alpha(t)$ in between 1 and 10 µs for the crowding ratios 1:75 and 1:50. For the highest crowding fraction $\alpha(t)$ reaches a minimum of around 0.6, indicating quite pronounced anomalous diffusion. As this feature is much less prominent for the non-aggregated system this drop in $\alpha(t)$ cannot be due to lipid–protein collisions as such. It appears plausible that the decrease of $\alpha(t)$ is mainly due to those lipid molecules whose motion is confined by protein cages. Indeed, Fig. 13 demonstrated the existence of such cages, which can also be identified in selected lipid trajectories [148]. The fact that $\alpha(t)$ eventually recovers the Brownian value of unity suggests that the caging is transient, and caged lipids at longer times are set free and resume more vivid motion [148].

For the protein motion shown in Fig. 16 we find a behaviour similar to the lipid motion. Generally, the absolute values of the local anomalous diffusion exponent is smaller than that for the lipid motion. Moreover, the dip in the value of $\alpha(t)$ occurs at later time scales, as is the crossover time to normal diffusion. The main difference is for the aggregating case: here the lipid motion does not exhibit the massive drop of $\alpha(t)$ as the lipid motion. This reflects the more homogeneous distribution of mobilities for the proteins, in contrast to the population splitting between free and caged lipids [148].

5.3.1. Non-Gaussian anomalous diffusion in protein-crowded membranes.

For the dilute bilayer system we found that the observed anomalous diffusion is governed by the fractional Langevin Eq. (16). This means that the motion becomes antipersistent, as evidenced in the negative cusp of the displacement autocorrelation function; see Fig. 9D. In particular, the motion we observed is of Gaussian nature. This character of the diffusion is preserved for the liquid phase bilayer in the presence of cholesterols as well as for the gel phase bilayer. Does crowding change this commonly assumed physical behaviour of the diffusion?

Extensive coarse grained simulations were performed in addition to those reported in Ref. [148]. The analysis corroborates the time variation of the anomalous scaling exponent, as reported above. Moreover, it confirms the population splitting into mobile and caged lipids. This causes a pronounced amplitude variation between individual time averaged mean squared displacements, the corresponding amplitude distribution $\phi(\xi)$, however, remains qualitatively consistent with fractional Langevin equation type motion. The width of the amplitude scatter decreases with the observation time. The displacement correlation function shows an antipersistency of the motion, however, there exists
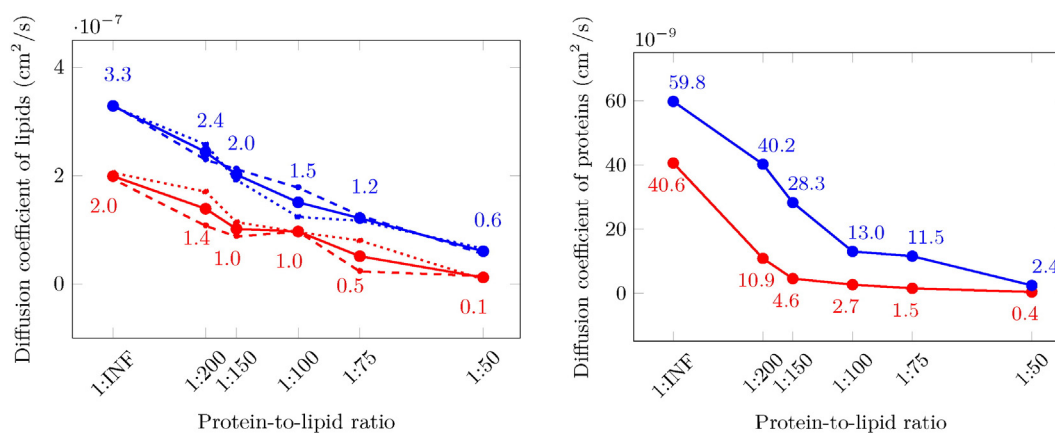

Fig. 14. Diffusion coefficients of lipid molecules (left) and embedded proteins (right) in membranes with different protein-to-lipid ratios. The data for the non-aggregating DLPC bilayer are shown in blue while red denotes the aggregating DPPC bilayer. INF stands for infinity, the dilute case with only one embedded protein. In the left panel the diffusion coefficients in x and y directions are denoted by dashed and dotted lines of the same colour, respectively, the full curve represents their average [148]. Note the different multiplication factors for the vertical scales.
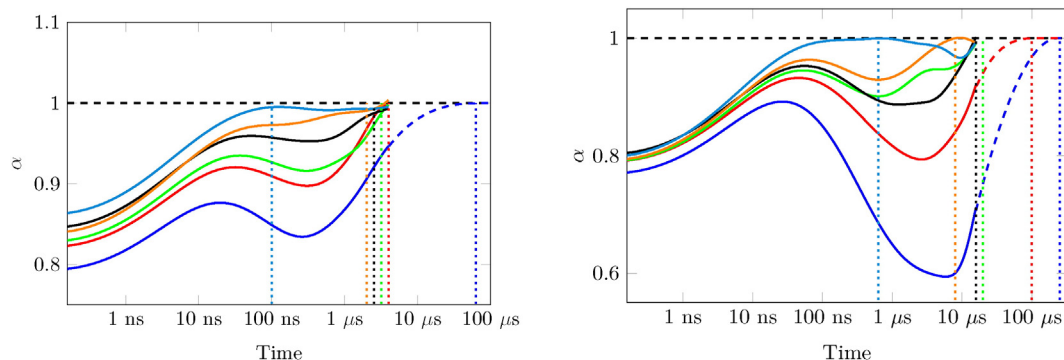
Fig. 15. Local anomalous diffusion exponent $\alpha(t)$ for the lipid motion in the non-aggregating (left) and aggregating (right) systems, colour-coded by: 1:50 (blue), 1:75 (red), 1:100 (green), 1:150 (black), 1:200 (orange), and 1:infinity (cyan). Extrapolations at the longest times (shown by dashed lines) are based on conservative estimates of $\alpha(t)$ between about 3–20 μs [148]. Approximate crossover times to normal diffusion are indicated by the vertical dotted lines.

some deviation from the correlation function obtained from the fractional Langevin equation [150].

The striking feature for the crowded systems is that the probability density function for both the lipid and protein motion *deviates from a Gaussian shape*. Instead the data show a consistent agreement with a stretched Gaussian form $P(r,t) \simeq \exp(-[r/(ct^{\alpha/2})]^{\delta})$, where the stretching exponent δ is found to vary within the range between 1.4 and 1.6 for the crowded system. The control shows that a fit of this function to the dilute case diffusion consistently reproduces the Gaussian value $\delta = 2$ [150]. This finding is poised to shake some of the accepted fundamental views of the motion of lipids and proteins in lipid bilayer systems.

6. Elastic response of elastic substrates

6.1. Particle diffusion, assembly, and electrostatics on membranes

In this section we briefly address the study of the elastic response of elastic substrates, which is gaining fresh momentum. We include this section as the physical properties discussed here may impact the lipid and protein motion in supporting membranes. The reader is referred here to the review of Matthias Weiss in this BBA special issue on lipid-mediated interactions of membrane bound proteins [104]. Membrane shape deformations due to protein crowding and segregation are also summarised there. Recent studies demonstrate how orientation dependent forces between individual filamentous fd bacteriophages adsorbed on freestanding cationic lipid DOPC-DOTAP membranes guide the relative positioning and assembly to higher structures of tohe virus [151].

Can we understand the formation of such aggregates, and, ultimately, its dynamics? In that process the membrane centreline undergoes *out of plane* deformations [152–156], as shown schematically in Fig. 17. As a first attempt we examine *in-plane* deformations of a responsive elastic substrate upon binding of a rod-like object. We

quantify the deformations of the elastic substrate as a response to the adhesion of filamentous particles and demonstrate that tip-to-tip contacts of rods are favoured for relatively soft substrates while side-to-side contacts become profitable for stiffer substrates. An example for our model system is shown in Fig. 18.

The phenomenon of aggregation and self-assembly were also observed experimentally for colloidal particles on giant phospholipid vesicles [157]. Another set of experimental observations stems from a recent study of linear versus side-by-side assembly of BAR proteins on elastic membranes—both in the absence and presence of external surface tension—as reported in Ref. [158], compare also Refs. [159, 160]. It was demonstrated by coarse grained molecular dynamics simulations that larger protein–membrane adhesion strength favours the end-to-end protein assembly, while progressively higher membrane tensions rather facilitate the formation of aggregates with side-by-side contacts [158].

The topics of assembly and pattern formation of colloidal particles of various shapes and surface properties on liquid interfaces are actively studied in colloidal science [161–164]. The analogy between the curvature mediated interactions of particles on membranes and capillary immersion interactions is relatively close [163,165–167]. The deformations of the neighbourhood of a particle immersed in a liquid scales with the liquid contact angle due to wetting. This is reminiscent of the lipid membrane deformations triggered by, for instance, electrostatic binding of oppositely charged DNA molecules [152] or rod-like viruses [151] as those model systems schematically shown in Fig. 18. The propensity of membrane wrapping around the particles scales with their mutual attraction strength. Meniscus-shape deformations for capillary interactions are similar to out-of-plane bending deformations of the membrane that trigger the aggregation of the adsorbed particles [151,163,164,168,169]. We note that the clustering of trans-membrane proteins was reviewed recently [170]. The hydrophobic mismatch of protein-like inclusions [171,172] gives rise to deformations of the membrane height with power-law decay of long-range forces along
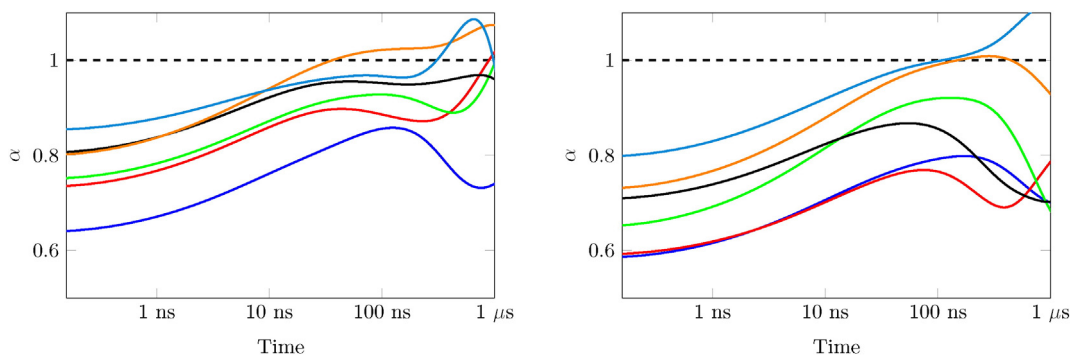

Fig. 16. Local anomalous diffusion exponent $\alpha(t)$ for the protein motion in the non-aggregating (left) and aggregating (right) systems. Colour coding is the same as in Fig. 15 [148].
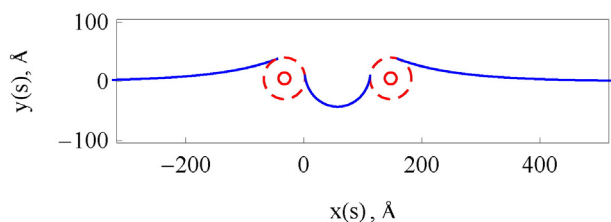
Fig. 17. A typical shape of a cationic membrane centreline hosting two parallel DNA rods [152]. Membrane-DNA wrapping is more pronounced for highly charged and elastically soft membranes.

the membrane. We also note that membrane-associated factories of some viruses—which utilise higher concentrations of virus capsid proteins and other components—employ a membrane-facilitated assembly strategy [173].

One physical mechanism of the linear assembly of rods is minimisation of the elastic energy—accumulated in particular around the particle tips—via connecting the tips on the membrane to reduce the portion of highly curved membrane surface area. Another reason—that might be relevant particularly at low salt solutions—are repulsive electrostatic interactions [174–176] between the highly negatively charged rod-like particles. For the rod-like particles in closely aligned side-by-side configurations the repulsion of their charges is evidently stronger than for a tip-to-tip arrangement [200]. For our brief discussion here we neglect charge mediated effects, focusing on membrane mediated forces.

We end this subsection with some remarks on the relevance of electrostatic effects on the diffusion and segregation behaviour in lipid membranes. First, we note that the diffusion of components on the surface of biological membranes are subject to highly compartmentalised, heterogeneous and often dynamic environment imposing various barriers for the particle motion [177]. In such settings charge-mediated interactions may, for instance, influence the particle diffusion on lipid membranes and monolayers in several different ways. For positively charged lipids the formation of clusters of lipids may be facilitated upon addition of divalent cations such as Mg^{2+} or Ca^{2+} into the system [180], thus effectively adding features of *crowding*. Moreover, the effective interactions of diffusing particles with membrane lipids and other larger membrane components may become affected, altering the dynamics of the relocation from one site to another along the membrane. Additionally, the effective size of the tracer might change due to clustering/adhesion of lipids onto its surface, provided that particle and lipids have opposite charges. Lastly, the effective membrane viscosity for the lateral particle motion may be affected by electric charges. The relative contribution of these effects will depend on the charges of the lipid and particle, the size of diffusing membrane bound particles, salt concentration, ambient temperature, etc.

The implications of electrostatic effects on membrane domain segregation, phase separation behaviour, and lateral diffusion of membrane components were examined, inter alia, in Refs. [178–180]. Experimentally, the diff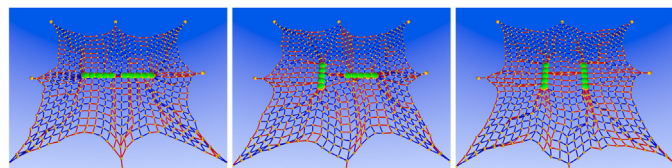usion properties on phase-separated membranes [180] (see also Ref. [181]) were shown to be sensitive functions of the domain size and particle interactions with the domains, with the effective domain diffusivity varying differently with the domain density for pure water versus solutions at nearly physiological salt conditions. Brownian long time diffusion of domains in Langmuir lipid monolayers was also shown to slow down with the domain density due to increasing intrinsic viscosity of the lipid layer [179]. For freestanding membranes, the translational diffusion of membrane bound negatively charged polystyrene beads of 10 nm size the diffusivity was approximately *independent* of the fraction of cationic lipids in the range of up 7% [182]. This indicates no measurable effect of the membrane charge density on its viscous properties [183].

In simulations, the diffusion properties on phase separated, heterogeneous two dimensional membranes were demonstrated to be severely affected by attractive dipole–dipole interactions of tracer particles to liquid-condensed membrane domains [178]. A stronger tracer-domain binding effectively renders the diffusion from two to one dimension, reducing also the long time diffusion coefficient in the Brownian limit, see also Ref. [184]. These conclusions about the particle confinement, anomalous diffusion on intermediate time scales, and localisation of the tracer particles are qualitatively similar to recent results for obstructed diffusion in three dimensional lattices of attractive crowders [79]. Note here that some raft-associated membrane proteins such as E-cadherin and neutral cell adhesion molecules are indeed known to possess large dipole moments [178].

Note that electrostatic fields emerging from the membrane surface—varied via changing the solution pH and salt concentration [185]—will also affect the diffusion of small molecules such as protons on the *outside* of lipid membranes. Finally, the effect of a low dielectric constant of the lipid layer and solution salinity on the strength of domain–domain electrostatic interactions was discussed in Ref. [180], see also Refs. [186–188] for a theoretical perspective on charge interactions along low-dielectric membranes. The reader is also referred to the studies [189–194] for general consideration of membrane electrostatics.

6.2. Rod-like particles on elastic substrates

From Langevin dynamics simulations the substrate mediated interactions between rod-like particles adsorbed onto a responsive elastic interface were investigated, using a discrete two-dimensional lattice-based model [195]. The bead–spring network lattice shown in Fig. 18 is of size n with $(n+1)^2$ beads, where n is varied in the range $15 < n < 25$, to minimise boundary effects. Each bead of the network is subject to fluctuations of the thermal bath. The entire film is anchored at eight points forming a pre-stretched elastic sheet. This maintains the shape of the sheet and prevents its collapse onto adsorbed attractive particles. Such a basal tension in the membranous network is typically non-zero for large membrane vesicles [151,182,196].

The overall binding energy E_A of a rod-like particle to surrounding network beads is supposed to mimic e.g. the interactions of filamentous viruses with oppositely charged membranes [151]. In the simulations the rods are represented by linear straight arrays of unit size spheres with total length l (in terms of the lattice constant a). The strength ε_A of the bead adhesion to each sphere is parametrised by the truncated 6–12 Lennard–Jones (LJ) potential [195,197]. The network beads interact by the standard Weeks–Chandler–Andersen repulsive potential [198,199].

We observe in Fig. 19 that the tip-to-tip configuration of the rods is favoured for very elastic membranes when the particles only feel each other over short distances. The absolute value of the interaction energy grows with the rod–membrane attraction energy. For rigid membranes and strong attraction the side-to-side contacts of rods become more favourable due to longer range membrane deformations and a longer overlap of deformed regions in this case. These results can be a testable prediction for future experiments.

Fig. 18. Schematics of adhesive rods positioned at various orientations on a responsive gel-like membrane interface. From left to right: the rods are in tip-to-tip orientation, in perpendicular arrangement, and in parallel side-to-side configuration. The red and blue colours of the network springs denote stretched and compressed links, respectively [200]. Image courtesy S. Ghosh.
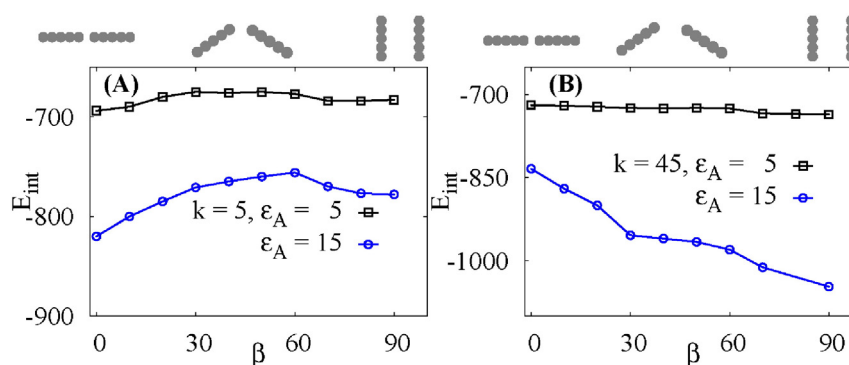
Fig. 19. Rod–rod membrane mediated interaction energy $E_{int}(\beta, d)$ in units of thermal energy versus the angle β of the mutual rotation. Parameters: the rod length is $l = 5a$ and the centre-to-centre distance is $d = 6a$ [200].

It will remain an interesting question to determine the exact dynamics of the pattern formation of the particles on a membrane. Concurrently, the effects on the diffusion of lipids close to the adsorbed particles and their indentations on the membrane will have to be examined.

7. Discussion and conclusions

Lipid membranes are effectively two-dimensional bilayers assembled from densely packed but still laterally highly mobile phospholipid molecules. The diffusion coefficients for the long time motion of lipids in fluid membranes vary in the range 1–20 μm^2/s, depending on the lipid type, ambient temperature, ionic strength of the buffer, and the lipid composition—native membranes contain a large variety of different lipid chemistries—[125,201]. Note that despite terming them as liquids membranes are up to 100 times more viscous than water [202]. This often gives rise to a collective motion of membrane proteins with a dozen of surrounding lipids [203,204].

The lipid membrane in biologically relevant systems is often highly crowded with membrane proteins, as shown in the computational models in Figs. 1 and 12. The protein-to-lipid ratio often varies in the range of 1:200–1:50 [96,141,96,142]. The specific level of crowding in membranes by proteins is maintained by cells to ensure a tradeoff with the optimal yield and kinetics of biochemical reactions on and across the membrane [205]. The study of the physical and biochemical pathways and assemblies of lipid molecules is often referred to as *lipidomics* [131] in recognition of their high importance for biological cells.

A substantial fraction of cell resident proteins is bound to outer cell membranes. The average spacing between proteins on the membrane is some 10 nm or less. The intrinsic heterogeneity of components, lipid demixing and membrane compartmentalisation are fundamental organisational principles of biomembranes, see Fig. 12. Membrane heterogeneities provide a handle for a cell to tune the activity of its functional components. Lipid microdomains affect the yield of membrane associated proteins participating in signalling pathways. The formation of such domains by electrostatic lipid–proteins interactions was demonstrated by simulations [206].

Such studies are intimately connected to the still elusive yet physiologically fundamental question concerning the formation as well as the very existence of *lipid rafts*, formally defined as microdomains of size 10 to 200 nm. Such rafts are believed to serve as organising centres for the assembly of signalling molecules. Rafts influence the membrane fluidity and thus impact on the trafficking of membrane proteins as well as regulating neurotransmission and receptor [207,208]. Lipid rafts are more ordered and tightly packed than the surrounding bilayer, but may float freely in the membrane bilayer [209]. The concept of lipid rafts goes back to the pioneering works of Stier, Sackmann, and others [210,211]. A more recent cornerstone towards the understanding of

lipid rafts is the work of Ikonen and Simons [220]. A slowing down of lipid diffusion in crowded membranes as considered in this review likely contributes to transport phenomena on cell membranes affecting the overall dynamics, in particular, the formation of lipid rafts [97,125,130, 217–223] and membrane domains [224].

The motion of specific membrane embedded proteins is also believed to be intimately connected to other physiological functions. For instance, the dynamics of so-called clathrin-mediated endocytosis were recently shown to be mediated by the anomalous diffusion of potassium channels in the cell membrane, giving rise to the highly heterogeneous distribution of lifetimes involved in the complex formation [87]. All these questions pose the need for a better understanding of the nature of a random, thermally driven motion of membrane lipids and embedded proteins over a wide range of time scales.

We here provide an overview over recent experimental results reporting anomalous diffusion of membrane embedded proteins in living biological cells. Apart from the sublinear scaling in time of the mean squared displacement the motion of several investigated membrane embedded proteins reveals the phenomenon of ageing, according to which the mobility of the proteins is a decreasing function of time [85]. This effects a population splitting into a fraction of proteins with varying mobility and another, immobile fraction. By advanced experimental techniques also the anomalous diffusion of membrane lipids was shown. We mention, however, that recent FCS studies of model membranes in the presence of membrane-bound actin cytoskeleton of varying concentration showed that although a considerable reduction of lipid and protein diffusivity was detected, no anomalous diffusion was observed [225]. The observation of anomalous diffusion on the intermediate and long time scales accessible to experiments therefore appears to depend on the very setting of the system under consideration. For a number of proteins embedded in the membranes of living biological cells it was unambiguously shown that anomalous diffusion persists over macroscopic time scales of the order of minutes [85,95].

The connection with cellular elements indeed adds another level of complexity to the dynamics of lipids and membrane proteins. Thus, the actin cytoskeleton adjacent to the membrane acts as constraining fences leading to a splitting into a faster diffusion within a compartment and a slower hop-like motion between the compartments [110,202], the effect being particularly pronounced for trans-membrane proteins. For plasma membranes the size of the compartments and the transition times between the compartments were measured in Ref. [226]. These experimental results are consistent with Monte Carlo simulations on plasma membranes [146]. For supported model lipid membranes transient anomalous diffusion on time scales below 20 ms was observed by single particle tracking and shown to be effected by oxide surface nanostructures [227]. A partial lipid immobilisation by membrane bound cytoskeletal filaments [212–214] has also been studied by simulations [215].

On much shorter time scales, we showed how massive computer simulations provide insight into the dynamics, spatiotemporal organisation, and response behaviour of model lipid membranes. We demonstrated the existence of anomalous diffusion of lipid molecules in various settings such as pure lipid bilayers in the liquid and gel phases as well as in the liquid phase in the presence of cholesterols. In all these cases our detailed analysis in terms of the mean squared displacement, the displacement correlation function, moment ratios, and the amplitude distribution function of the time averaged mean squared displacement demonstrated that the anomalous dynamics are Gaussian in nature and can be described in terms of a generalised Langevin equation with power-law memory, driven by Gaussian noise with long-range temporal correlations. Anomalous diffusion was also shown to exist in protein-crowded lipid bilayers for both the lipids and the membrane embedded proteins. Remarkably, however, it is found that the diffusion of both lipids and proteins in crowded systems is no longer Gaussian but in good agreement with *stretched Gaussian shapes* of the distribution function [150].

In pure lipid bilayers anomalous diffusion only persists up to a crossover time of around 10 ns, beyond which normal Brownian motion emerges. In the presence of cholesterol we saw that certain lipid chemistries still show normal diffusion beyond this crossover time whereas persisting anomalous diffusion was found for other chemistries. In the gel phase of a pure lipid bilayer the short time anomalous diffusion is characterised by an extremely low anomalous diffusion exponent, and anomalous diffusion also exists beyond the crossover time. In these systems it was shown that the lipid motion corresponds to a concerted dance of a whole neighbourhood, in contrast to the classical hop diffusion picture. Differences between the long time diffusivities and the intermediate time anomalous diffusion in these simple systems is mainly due to the detailed chemistry of the lipids and their available space in the bilayer.

In contrast to this the lipid and protein motion is more complex in crowded bilayer systems relevant to living biological cells. The exact nature of the observed non-Gaussian anomalous diffusion process remains elusive. At least for the lipid motion a very similar behaviour is observed for the motion of finite sized particles in arrays of obstacles, even at a relatively low obstacle density [150]. We may therefore speculate whether some of the anomalous diffusion features observed here in fact have a quite generic physical origin and are independent of the complicated structural details of the involved proteins and lipids. One of the greatest challenges in membrane biophysics is to understand the dynamics of membrane components and the response of biomembranes to the binding of various macromolecules and proteins [228–230]. Modern superresolution microscopy techniques and massive computer simulations open up an increasingly large window to study these questions.

The high performance of supercomputer simulations—with the enormous level of detail of lipids and membrane bound proteins, with explicit water, and specific interactions between the component—often surpasses analytical studies of model and simplified lipid membranes. This renders computer simulations the main tool for the theoretical understanding of the dynamics and functioning principles of biological membranes. This is particularly true for multicomponent, intrinsically heterogeneous and crowded, but still highly dynamic real cell membranes, in particular, also in the presence of underlying cytoskeletal structures.

Conflict of interest

The authors declare no conflict of interest.

Transparency document

The Transparency document associated with this article can be found, in online version.

References

[1] M.V. Smoluchowski, Phys. Z. 17 (1916) 557.
[2] N.G. van Kampen, Stochastic Processes in Physics and Chemistry, Elsevier, Amsterdam, 2007.
[3] C. Loverdo, O. Bénichou, M. Moreau, R. Voituriez, Nat. Phys. 9 (2008) 134.
[4] A. Godec, R. Metzler, Phys. Rev. E 92 (2015) 010701(R).
[5] P.H.V. Hippel, O.G. Berg, J. Biol. Chem. 264 (1989) 675.
[6] M. Bauer, R. Metzler, PLoS ONE 8 (2013) e53956;
    O. Pulkkinen, R. Metzler, Phys. Rev. Lett. 110 (2013) 198101.
[7] A.B. Kolomeisky, Phys. Chem. Chem. Phys. 13 (2011) 2088;
    M. Sheinman, O. Bénichou, Y. Kafri, R. Voituriez, Rep. Prog. Phys. 75 (2012) 026601.
[8] M.J. Saxton, K. Jacobsen, Annu. Rev. Biophys. Biomol. Struct. 26 (1997) 373.
[9] F. Höfling, T. Franosch, Rep. Prog. Phys. 76 (2013) 046602.
[10] C. Manzo, M.F. Garcia-Parajo, Rep. Prog. Phys. 78 (2015) 124601.
[11] R. Metzler, J. Klafter, Phys. Rep. 339 (2000) 1.
[12] E. Barkai, Y. Garini, R. Metzler, Phys. Today 65 (8) (2012) 29.
[13] R. Metzler, J.-H. Jeon, A.G. Cherstvy, E. Barkai, Phys. Chem. Chem. Phys. 16 (2014) 24128.
[14] Y. Meroz, I.M. Sokolov, Phys. Rep. 573 (2015) 1.
[15] S. Condamin, V. Tejedor, R. Voituriez, O. Benichou, J. Klafter, Proc. Natl. Acad. Sci. U. S. A. 105 (2008) 5675.
[16] M. Magdziarz, A. Weron, K. Burnecki, J. Klafter, Phys. Rev. Lett. 103 (2009) 180602.
[17] V. Tejedor, O. Benichou, R. Voituriez, R. Jungmann, F. Simmel, C. Selhuber-Unkel, L. Oddershede, R. Metzler, Biophys. J. 98 (2010) 1364.
[18] A. Robson, K. Burrage, M.C. Leake, Philos. Trans. R. Soc. B 368 (2012) 20120029.
[19] D. Ernst, J. Köhler, M. Weiss, Phys. Chem. Chem. Phys. 16 (2014) 7686.
[20] E. Kepten, A. Weron, G. Sikora, K. Burnecki, Y. Garini, PLoS ONE 10 (2015) e0117722.
[21] R.H. Austin, et al., Biochemistry 14 (1975) 5355.
[22] H.P. Lu, L. Xun, X.S. Xie, Science 282 (1998) 1877.
[23] X. Hu, L. Hong, M.D. Smith, T. Neusius, X. Cheng, J.C. Smith, Nat. Phys. 12 (2016) 171.
[24] S. Takamori, M. Holt, K. Stenius, E.A. Lemke, M. Grønborg, D. Riedel, H. Urlaub, S. Schenck, B. Brügger, P. Ringler, S.A. Müller, B. Rammner, F. Gräter, J.S. Hub, B.L. de Groot, G. Mieskes, Y. Moriyama, J. Klingauf, H. Grubmüller, J. Heuser, F. Wieland, R. Jahn, Cell 127 (2006) 831.
[25] I. Golding, E.C. Cox, Phys. Rev. Lett. 96 (2006) 098102.
[26] A.R. McGuffee, A.H. Elcock, PLoS Comput. Biol. 6 (2010) e1000694.
[27] F. Trovato, V. Tozzini, Biophys. J. 107 (2014) 2579.
[28] S.B. Zimmerman, A.P. Minton, Annu. Rev. Biophys. Biomol. Struct. 22 (1993) 27.
[29] H.X. Zhou, G. Rivas, A.P. Minton, Annu. Rev. Biophys. 37 (2008) 375.
[30] H.X. Zhou, J. Mol. Recognit. 17 (2004) 368.
[31] M. Weiss, Int. Rev. Cell Mol. Biol. 307 (2014) 383.
[32] A.R. Denton, Int. Rev. Cell Mol. Biol. 307 (2014) 27.
[33] M. Yanagisawa, T. Sakaue, K. Yoshikawa, Int. Rev. Cell Mol. Biol. 307 (2014) 175.
[34] K.A. Dill, K. Ghosh, J.D. Schmit, Proc. Natl. Acad. Sci. U. S. A. 108 (2011) 17876.
[35] N.A. Denesyuk, D. Thirumalai, J. Am. Chem. Soc. 133 (2011) 11858.
[36] O. Stiehl, K. Weidner-Hertrampf, M. Weiss, New J. Phys. 15 (2013) 113010.
[37] J. Shin, A.G. Cherstvy, R. Metzler, Soft Matter 11 (2015) 472.
[38] G. Schreiber, G. Haran, H.-X. Zhou, Chem. Rev. 109 (2009) 839.
[39] A.P. Minton, Curr. Opin. Struct. Biol. 10 (2000) 34.
[40] M.S. Cheung, D. Klimov, D. Thirumalai, Proc. Natl. Acad. Sci. U. S. A. 102 (2005) 4753.
[41] A.P. Minton, Biophys. J. 88 (2005) 971.
[42] A.P. Minton, J. Pharm. Sci. 94 (2005) 1668.
[43] R.J. Ellis, A.P. Minton, Biol. Chem. 387 (2006) 485.
[44] J. Schoeneberg, A. Ullrich, F. Noe, BMC Biophys. 7 (2014) 11.
[45] P. Schwille, U. Haupts, S. Maiti, W.W. Webb, Biophys. J. 77 (1999) 2251.
[46] P. Schwille, J. Korlach, W.W. Webb, Cytometry 36 (1999) 176.
[47] M. Weiss, M. Elsner, F. Kartberg, T. Nilsson, Biophys. J. 87 (2004) 3518.
[48] S.C. Weber, A.J. Spakowitz, J.A. Theriot, Phys. Rev. Lett. 104 (2010) 238102.
[49] T. Lebeaupin, H. Sellou, G. Timinszky, S. Huet, AIMS Biophys. 2 (2015) 458.
[50] I. Bronstein, Y. Israel, E. Kepten, S. Mai, Y. Shav-Tal, E. Barkai, Y. Garini, Phys. Rev. Lett. 103 (2009) 018102.
[51] I.M. Tolić-Nørrelykke, E.-L. Munteanu, G. Thon, L. Oddershede, K. Berg-Sørensen, Phys. Rev. Lett. 93 (2004) 078102.
[52] J.-H. Jeon, V. Tejedor, S. Burov, E. Barkai, C. Selhuber-Unke, K. Berg-Soerensen, L. Oddershede, R. Metzler, Phys. Rev. Lett. 106 (2011) 048103.
[53] S.M.A. Tabei, S. Burov, H.Y. Kim, A. Kuznetsov, T. Huynh, J. Jureller, L.H. Philipson, A.R. Dinner, N.F. Scherer, Proc. Natl. Acad. Sci. U. S. A. 110 (2013) 4911.
[54] J. Vercammen, G. Martens, Y. Engelborghs, Springer Ser. Fluoeresc. 4 (2007) 323.

[55] G. Seisenberger, M.U. Ried, T. Endreß, H. Büning, M. Hallek, C. Bräuchle, Science 294 (2001) 1929.
[56] G. Guigas, M. Weiss, Biophys. J. 94 (2008) 90.
[57] J. Szymanski, M. Weiss, Phys. Rev. Lett. 103 (2009) 038102.
[58] W. Pan, L. Filobelo, N.D.Q. Pham, O. Galkin, V.V. Uzunova, P.G. Vekilov, Phys. Rev. Lett. 102 (2009) 058101.
[59] J.-H. Jeon, N. Leijnse, L.B. Oddershede, R. Metzler, New J. Phys. 15 (2013) 045011.
[60] J. Mattsson, H.M. Wyss, A. Fernandez-Nieves, K. Miyazaki, Z. Hu, D.R. Reichman, D.A. Weitz, Nature 462 (2009) 83.
[61] I.Y. Wong, M.L. Gardel, D.R. Reichman, E.R. Weeks, M.T. Valentine, A.R. Bausch, D.A. Weitz, Phys. Rev. Lett. 92 (2004) 178101.
[62] E.R. Weeks, J.C. Crocker, A.C. Levitt, A. Schofield, D.A. Weitz, Science 287 (2000) 627.
[63] A. Godec, M. Bauer, R. Metzler, New J. Phys. 16 (2014) 092002.
[64] D. Robert, T.H. Nguyen, F. Gallet, C. Wilhelm, PLoS ONE 4 (2010) e10046.
[65] I. Goychuk, V.O. Kharchenko, R. Metzler, PLoS ONE 9 (2014) e91700;
Phys. Chem. Chem. Phys. 16 (2014) 16524.
[66] B. Wang, J. Kuo, S.C. Bae, S. Granick, Nat. Mater. 11 (2012) 481.
[67] J.F. Reverey, J.-H. Jeon, M. Leippe, R. Metzler, C. Selhuber-Unkel, Sci. Rep. 5 (2015) 11690.
[68] C. die Rienzo, et al., Nat. Commun. 5 (2014) 5891.
[69] M.G. Del Popolo, G.A. Voth, J. Phys. Chem. B 108 (2004) 1744.
[70] F. Höfling, T. Franosch, Rep. Prog. Phys. 76 (2013) 046602.
[71] J.-H. Jeon, H.M. Monne, M. Javanainen, R. Metzler, Phys. Rev. Lett. 109 (2012) 188103.
[72] S. Burov, R. Metzler, E. Barkai, Proc. Natl. Acad. Sci. U. S. A. 107 (2010) 13228.
[73] I.M. Zaid, M.A. Lomholt, R. Metzler, Biophys. J. 97 (2009) 710;
M.A. Lomholt, I.M. Zaid, R. Metzler, Phys. Rev. Lett. 98 (2007) 200603.
[74] G. Bel, E. Barkai, Phys. Rev. Lett. 94 (2005) 240602;
G. Bel, E. Barkai, Phys. Rev. E 73 (2006) 016125;
A. Rebenshtok, E. Barkai, Phys. Rev. Lett. 99 (2007) 210601.
[75] Y. He, S. Burov, R. Metzler, E. Barkai, Phys. Rev. Lett. 101 (2008) 058101.
[76] J.-H. Jeon, R. Metzler, J. Phys. A 43 (2010) 252001.
[77] S.M. Rytov, Yu.A. Kravtsov, V.I. Tatarskii, Principles of Statistical Radiopysics 1: Elements of Random Process Theory, Springer, Heidelberg, 1987.
[78] W. Deng, E. Barkai, Phys. Rev. E 79 (2009) 011112.
[79] S.K. Ghosh, A.G. Cherstvy, R. Metzler, Phys. Chem. Chem. Phys. 17 (2015) 1847.
[80] L.C.E. Struik, Physical Aging in Amorphous Polymers and Other Materials, Elsevier, Amsterdam, 1978;
E.J. Donth, The Glass Transition, Springer, Berlin, 2001;
W. Götze, Complex Dynamics of Glass-forming Liquids: a Mode-coupling Theory, Oxford University Press, Oxford, UK, 2009.
[81] E. Bertin, J.-P. Bouchaud, Phys. Rev. E 67 (2003) 026128;
C. Monthus, J.-P. Bouchaud, J. Phys. A 29 (1996) 3847;
S. Burov, E. Barkai, Phys. Rev. Lett. 98 (2007) 250601.
[82] J.H.P. Schulz, E. Barkai, R. Metzler, Phys. Rev. Lett. 110 (2013) 020602;
Phys. Rev. X 4 (2014) 011028.
[83] P.G. Saffman, M. Delbrück, Proc. Natl. Acad. Sci. U. S. A. 72 (1975) 3111.
[84] M. Weiss, H. Hashimoto, T. Nilsson, Biophys. J. 84 (2003) 4043.
[85] A.V. Weigel, B. Simon, M.M. Tamkun, D. Krapf, Proc. Natl. Acad. Sci. U. S. A. 108 (2011) 6438.
[86] A. Lubelski, I.M. Sokolov, J. Klafter, Phys. Rev. Lett. 100 (2008) 250602.
[87] A.V. Weigel, M.M. Tamkun, D. Krapf, Proc. Natl. Acad. U. S. A. 110 (2013), E4591.
[88] H. Scher, E.W. Montroll, Phys. Rev. B 12 (1975) 2455.
[89] A.G. Cherstvy, A.V. Chechkin, R. Metzler, New J. Phys. 15 (2013) 083039;
J. Phys. A 47 (2014) 485002;
Soft Matter 10 (2014) 1591.
[90] A.G. Cherstvy, R. Metzler, J. Stat. Mech. (2015) P05010;
Phys. Rev. E 90 (2014) 012134;
Phys. Chem. Chem. Phys. 15 (2013) 20220.
[91] P. Massignan, C. Manzo, J.A. Torreno-Pina, M.F. Garca-Parako, M. Lewenstein, G.L. Lapeyre Jr., Phys. Rev. Lett. 112 (2014) 150603.
[92] J.-H. Jeon, A.V. Chechkin, R. Metzler, Phys. Chem. Chem. Phys. 16 (2014) 15811.
[93] A. Bodrova, A.V. Chechkin, A.G. Cherstvy, R. Metzler, Phys. Chem. Chem. Phys. 17 (2015) 21791;
New J. Phys. 17 (2015) 063038.
[94] M. Warren, J. Rottler, Phys. Rev. Lett. 110 (2013) 025501;
J. Helfferich, F. Ziebert, S. Frey, H. Meyer, J. Farago, A. Blumen, J. Baschnagel, Phys. Rev. E 89 (2014) 042604.
[95] C. Manzo, et al., Phys. Rev X 5 (2015) 011021.
[96] A.D. Dupuy, D.M. Engelman, Proc. Natl. Acad. Sci. U. S. A. 105 (2008) 2848.
[97] D. Krapf, Curr. Top. Membr. 75 (2015) 167.
[98] R. Phillips, T. Ursell, P. Wiggins, P. Sens, Nature 459 (2009) 379.
[99] D. Krapf, G. Campagnola, K. Nepal, and O. B. Peersen, (E-print arXiv: 1601.04198).
[100] A.V. Chechkin, I.M. Zaid, M.A. Lomholt, I.M. Sokolov, R. Metzler, Phys. Rev. E 86 (2012) 041101.
[101] C. Eggeling, et al., Nature 457 (2009) 1159.
[102] A. Honigmann, V. Müller, S.W. Hell, C. Eggeling, Faraday Discuss. 161 (2013) 77.
[103] C.L. Armstrong, M. Trapp, J. Peters, T. Seydel, M.C. Rheinstädter, Soft Matter 7 (2011) 8358.
[104] G. Guigas and M. Weiss, Biochim. Biophys. Acta Biomembr., http://dx.doi.org/10.1016/j.bbamem.2015.12.021.
[105] E. Flenner, J. Das, M.C. Rheinstädter, I. Kosztin, Phys. Rev. E 79 (2009) 011907.
[106] W.L.C. Vaz, R.M. Clegg, D. Hallman, Biochem. J. 24 (1985) 781;
P.F.F. Almeida, W.L.C. Vaz, T.E. Thompson, Biochem. J. 31 (1992) 6739.
[107] W.L.C. Vaz, R.M. Clegg, D. Hallman, Biochemistry 24 (1985) 781.
[108] P.F.F. Almeida, W.L.C. Vaz, T.E. Thompson, Biochemistry 31 (1992) 6739.
[109] W.L.C. Vaz, P.F. Almeida, Biophys. J. 60 (1991) 1553.
[110] T. Fujiwara, K. Ritchie, H. Murakoshi, K. Jacobson, A. Kusumi, J. Cell Biol. 157 (2002) 1071.
[111] E. Falck, T. Rog, M. Karttunen, I. Vattulainen, J. Am. Chem. Soc. 130 (2008) 44.
[112] S. Busch, C. Smuda, L.C. Pardo, T. Unruh, J. Am. Chem. Soc. 132 (2010) 3232.
[113] G.R. Kneller, K. Baczynski, M. Pasenkiewicz-Gierula, J. Chem. Phys. 135 (2011) 141105.
[114] S. Stachura, G.R. Kneller, J. Chem. Phys. 40 (2014) 245.
[115] G.R. Kneller, J. Chem. Phys. 134 (2011) 224106;
J. Chem. Phys. 141 (2014) 041105.
[116] E. Lutz, Phys. Rev. E 64 (2001) 051106.
[117] R. Kubo, Rep. Prog. Phys. 29 (1966) 255.
[118] I. Goychuk, Phys. Rev. E 80 (2009) 046125;
Adv. Chem. Phys. 150 (2012) 187.
[119] P. Hänggi, Z. Phys. B 31 (1978) 407;
P. Hänggi, F. Mojtabai, Phys. Rev. E 26 (1982) 1168.
[120] S.C. Kou, Ann. Appl. Stat. 2 (2008) 501.
[121] T. Akimoto, et al., Phys. Rev. Lett. 107 (2011) 178103.
[122] E. Yamamoto, T. Akimoto, M. Yasui, K. Yasuoka, Sci. Rep. 4 (2014) 4720.
[123] L. Toppozini, F. Roosen-Runge, R.I. Bewley, R.M. Dalgliesh, T. Perring, T. Seydel, H.R. Glyde, V. García Sakai, M.C. Rheinstädter, Soft Matter 11 (2015) 8354.
[124] M.G. Wolf, H. Grubmüller, G. Groenhof, Biophys. J. 107 (2014) 76.
[125] N. Kahya, P. Schwille, Mol. Membr. Biol. 23 (2006) 29.
[126] J.J. Sieber, et al., Science 317 (2007) 1072.
[127] S.W.I. Siu, R. Vacha, P. Jungwirth, R.A. Böckmann, J. Chem. Phys. 128 (2008) 125103.
[128] H. Martinez-Seara, T. Rog, M. Karttunen, I. Vattulainen, R. Reigada, PLoS ONE 5 (2010), e11162.
[129] T. Vuorela, et al., PLoS Comput. Biol. 6 (2010), e1000964.
[130] A.J. Garcia-Saez, P. Schwille, FEBS Lett. 584 (2010) 1653.
[131] A. Shevchenko, K. Simons, Nat. Rev. Mol. Cell Biol. 11 (2010) 593.
[132] C. Hunte, S. Richers, Curr. Opin. Struct. Biol. 18 (2008) 406.
[133] Y. Schweitzer, M.M. Kozlov, PLoS Comput. Biol. 11 (2015), e1004054.
[134] C.L. Armstrong, W. Häußler, T. Seydel, J. Katsaras, M.C. Rheinstädter, Soft Matter 10 (2014) 2600.
[135] S. Meinhardt, R.L.C. Vink, F. Schmid, Proc. Natl. Acad. Sci. U. S. A. 110 (2013) 4476.
[136] T. Apajalahti, P. Niemelä, P. Govindan, M.S. Miettinen, E. Salonen, S.-J. Marrink, I. Vattulainen, Faraday Discuss. 144 (2010) 411.
[137] H. Martinez-Seara, et al., Biophys. J. 95 (2008) 3295.
[138] T. Heimburg, Thermal Biophysics of Membranes, Weinheim, Wiley VCH, 2007.
[139] S. Komura, D. Andelman, Adv. Colloid Interf. Sci. 208 (2014) 34.
[140] J. Ehrig, E.P. Petrov, P. Schwille, New J. Phys. 13 (2011) 045019.
[141] W.F.D. Bennett, D.P. Tieleman, Biochim. Biophys. Acta (BBA) - Biomembranes, 1828, 2013, 1765, D. Lingwood, H.-J. Kaiser, I. Levental, K. Simons (Eds.), Biochem. Soc. Trans. 37 (2009) 955.
[142] K. Jacobson, O.G. Mouritsen, R.G.W. Anderson, Nat. Cell Biol. 9 (2007) 7.
[143] M. Frick, K. Schmidt, B.J. Nichols, Curr. Biol. 17 (2007) 462.
[144] S. Wieser, J. Weghuber, M. Sams, H. Stockinger, G.J. Schutz, Soft Matter 5 (2009) 3287.
[145] V. Mueller, C. Ringemann, A. Honigmann, G. Schwartzmann, R. Medda, M. Leutenegger, S. Polyakova, V.N. Belov, S.W. Hell, C. Eggeling, Biophys. J. 101 (2011) 1651.
[146] K. Ritchie, X.-Y. Shan, J. Kondo, K. Iwasawa, T. Fujiwara, A. Kusumi, Biophys. J. 88 (2005) 2266.
[147] J.E. Goose, M.S.P. Sansom, PLoS Comput. Biol. 9 (2013), e1003033.
[148] M. Javanainen, H. Hammaren, L. Monticelli, J.-H. Jeon, M.S. Miettinen, H. Martinez-Seara, R. Metzler, I. Vattulainen, Faraday Discuss. 161 (2013) 397.
[149] M.P. Horton, F. Höfling, J.O. Radler, T. Franosch, Soft Matter 6 (2010) 2648.
[150] J.-H. Jeon, M. Javanainen, H. Martinez-Seara, R. Metzler, and I. Vattulainen (unpublished).
[151] A. Artemieva, C. Herold, E.P. Petrov, (unpublished); A. Artemieva, Interaction of fd-virus particles with cationic lipid membranes, Master Thesis, TU Dresden, 2013.
[152] A.G. Cherstvy, E.P. Petrov, Phys. Chem. Chem. Phys. 16 (2014) 2020.
[153] S. Dasgupta, T. Auth, G. Gompper, Nano Lett. 14 (2014) 687.
[154] A.H. Bahrami, R. Lipowski, T.R. Weikl, Phys. Rev. Lett. 109 (2012) 188102.
[155] A.H. Bahrami, et al., Adv. Colloid Interf. Sci. 208 (2014) 214.
[156] J. Agudo-Canalejo, R. Lipowsky, ACS Nano 9 (2015) 3704.
[157] I. Koltover, J.O. Rädler, C.R. Safinya, Phys. Rev. Lett. 82 (1999) 1991.
[158] M. Simunovic, G.A. Voth, Nat. Commun. 6 (2015) 7219.
[159] M. Simunovic, G.A. Voth, A. Callan-Jones, P. Bassereau, Trends Cell Biol. 25 (2015) 780.
[160] M. Simunovic, A. Srivastava, G.A. Voth, Proc. Natl. Acad. Sci. U. S. A. 110 (2013) 20396.
[161] J.C. Loudet, A.M. Alsayed, J. Zhang, A.G. Yodh, Phys. Rev. Lett. 94 (2005) 018301.
[162] J.C. Loudet, B. Pouligny, EPL 85 (2009) 28003.
[163] G.B. Davies, T. Krueger, P.V. Coveney, J. Harting, F. Bresme, Adv. Mater. 26 (2014) 6715.
[164] A. Saric, A. Cacciuto, Soft Matter 9 (2013) 6677.
[165] L. Botto, E.P. Lewandowski, M. Cavallaro Jr., K.J. Stebe, Soft Matter 8 (2012) 9957.
[166] M. Cavallaro Jr., L. Botto, E.P. Lewandowski, M. Wang, K.J. Stebe, Proc. Natl. Acad. Sci. U. S. A. 108 (2011) 20923.
[167] E.P. Lewandowski, J.A. Bernate, A. Tseng, P.C. Searson, K.J. Stebe, Soft Matter 9 (2009) 886.
[168] H. Tang, H. Ye, H.W. Zhang, Y. Zheng, Soft Matter 11 (2015) 8674.

[169] E.P. Lewandowski, M. Cavallaro Jr., I. Botto, J.C. Bernate, V. Garbin, K.J. Stebe, Langmuir 26 (2010) 15142.
[170] U. Schmidt, G. Guigas, M. Weiss, Phys. Rev. Lett. 101 (2008) 128104.
[171] P. Wiggins, R. Phillips, Biophys. J. 88 (2005) 880.
[172] T. Auth, G. Gompper, Phys. Rev. E 80 (2009) 031901.
[173] A. Zlotnick, personal communication (2013).
[174] S.L. Brenner, V.A. Parsegian, Biophys. J. 14 (1974) 327.
[175] A.G. Cherstvy, Phys. Chem. Chem. Phys. 13 (2011) 9942.
[176] A.A. Kornyshev, D.J. Lee, S. Leikin, A. Wynveen, Rev. Mod. Phys. 79 (2007) 943.
[177] W.S. Trimble, S. Grinstein, J. Cell Biol. 208 (2015) 259.
[178] M. Forstner, D. Martin, F. Rückerl, J. Käs, C. Selle, Phys. Rev. E 77 (2008) 051906.
[179] N. Wilke, B. Maggio, J. Phys. Chem. B 113 (2009) 12844.
[180] N. Wilke, B. Maggio, Biophys. Rev. 3 (2011) 185.
[181] T.V. Ratto, M.L. Longo, Biophys. J. 83 (2002) 3380.
[182] C. Herold, P. Schwille, E.P. Petrov, Phys. Rev. Lett. 104 (2010) 148102.
[183] E.P. Petrov, Pers. Commun. (2016).
[184] J.T. Mika, B. Poolman, Curr. Opin. Biotechnol. 22 (2011) 117.
[185] D.S. Alvares, M.L. Fanani, J.R. Neto, N. Wilke, Biochim. Biophys. Acta Biomembr. 1858 (2016) 393.
[186] D. Walther, P. Kuzmin, E. Donath, Eur. Biophys. J. 24 (1996) 125.
[187] R.R. Netz, Phys. Rev. E 60 (1999) 3174.
[188] A.G. Cherstvy, J. Phys. Chem. B 111 (2007) 7914 (and references cited therein).
[189] S. McLaughlin, Annu. Rev. Biophys. Biophys. Chem. 18 (1989) 113.
[190] G. Cevc, Biochim. Biophys. Acta 1031–3 (1990) 311.
[191] D. Andelman, Electrostatic properties of membranes: the Poisson–Boltzmann theory, Ch. 12, in: R. Lipowsky, E. Sackmann (Eds.), Handbook of Biological Physics, Elsevier 1995, pp. 603–641.
[192] R. Lipowsky, Generic interactions of flexible membranes, Ch. 11, in: R. Lipowsky, E. Sackmann (Eds.), Handbook of Biological Physics, Elsevier 1995, pp. 521–602.
[193] H. Boroudjerdi, Y.-W. Kim, A. Naji, R.R. Netz, X. Schlagberger, A. Serr, Phys. Rep. 416 (2005) 129.
[194] M. Langner, K. Kubica, Chem. Phys. Lipids, 101, 1999, 3; H. Brockman, Chem. Phys. Lipids, 73 (1994) 57.
[195] S. Ghosh, A.G. Cherstvy, R. Metzler, J. Chem. Phys. 141 (2014) 074903.
[196] C. Herold, P. Schwille, E.P. Petrov, J. Phys, D: Appl, Phys. 49 (2016) 074001.
[197] J. Shin, A.G. Cherstvy, R. Metzler, Phys Rev. X 4 (2014) 021002.
[198] J.D. Weeks, D. Chandler, H.C. Andersen, J. Chem. Phys. 54 (1971) 5237.
[199] M.P. Allen, D.J. Tildesley, Computer Simulations of Liquids, Clarendon Press, Oxford UK, 1987.
[200] S. Ghosh, A. G. Cherstvy, E. P. Petrov, and R. Metzler (unpublished).
[201] L. Bagatolli, P.B.S. Kumar, Soft Matter 5 (2009) 3234.
[202] A. Kusumi, et al., Annu. Rev. Biophys. Biomol. Struct. 34 (2005) 351.
[203] P.S. Niemela, M. Miettinen, L. Monticelli, H. Hammaren, P. Bjelkmar, T. Murtola, E. Lindahl, I. Vattulainen, J. Am. Chem. Soc. 132 (2010) 7574.
[204] M. Javanainen, et al., Langmuir 26 (2010) 15436.
[205] M. Hellmann, D.W. Heermann, M. Weiss, EPL 94 (2011) 18002.
[206] G. van den Bogaart, et al., Nature 479 (2011) 552.
[207] Z. Korade, A.K. Kenworthy, Neuropharmacology 55 (2008) 1265.
[208] L.J. Pike, J. Lipid Res. 50 (2008) S323.
[209] K. Simons, R. Ehehalt, J. Clin. Investig. 110 (2002) 597.
[210] A. Stier, E. Sackmann, Biochim. Biophys. Acta Biomembr. 311 (1973) 400.
[211] M.J. Karnovsky, A.M. Kleinfeld, R.L. Hoover, R.D. Klausner, J. Cell Biol. 94 (1982) 1.
[212] E.H. Zhou, F.D. Martinez, J.J. Fredberg, Nat. Mater. 12 (2013) 184; M. Baum, F. Erdel, M. Wachsmuth, K. Rippe, Nat. Comm. 5 (2014) 4494.
[213] E. Moeendarbary, et al., Nat. Mater. 12 (2013) 253.
[214] O. Lieleg, J. Kayser, G. Brambilla, L. Cipelletti, A.R. Bausch, Nat. Mater. 10 (2011) 236.
[215] E. Ehrig, E.P. Petrov, P. Schwille, Biophys. J. 100 (2011) 80.
[216] Y. von Hansen, S. Gekle, R.R. Netz, Phys. Rev. Lett. 111 (2013) 118103.
[217] E. Sezgin, et al., Biochim. Biophys. Acta 1818 (2012) 1777.
[218] K. Simons, J.L. Sampaio, Cold Spring Harb. Perspect. Biol. 3 (2011) a004697.
[219] K. Simons, W.L.C. Vaz, Annu. Rev. Biophys. Biomol. Struct. 33 (2004) 269.
[220] K. Simons, E. Ikonen, Nature 387 (1997) 569.
[221] K. Simons, D. Toomre, Nat. Rev. Mol. Cell Biol. 1 (2000) 31.
[222] D. Lingwood, K. Simons, Science 327 (2010) 46.
[223] K. Simons, M.J. Gerl, Nat. Rev. Mol. Cell Biol. 11 (2010) 688.
[224] E.P. Petrov, R. Petrosyan, P. Schwille, Soft Matter 8 (2012) 7552.
[225] F. Heinemann, S.K. Vogel, P. Schwille, Biophys. J. 104 (2013) 1465.
[226] K. Murase, T. Fujiwara, Y. Umemura, K. Suzuki, R. Iino, H. Yamashita, M. Saito, H. Murakoshi, K. Ritchie, A. Kusumi, Biophys. J. 86 (2004) 4075.
[227] R. Tero, G. Sazaki, T. Ujihara, T. Urisu, Langmuir 27 (2011) 9662.
[228] C. Yolcu, M. Deserno, Phys. Rev. E 86 (2012) 031906.
[229] B.J. Reynwar, G. Illya, V.A. Harmandaris, M.M. Müller, K. Kremer, M. Deserno, Nature 447 (2007) 461.
[230] T. Murtola, A. Bunker, I. Vattulainen, M. Deserno, M. Karttunen, Phys. Chem. Chem. Phys. 11 (2009) 1869.